Title of Document:

CONCUSSION: EXAMINING THE EFFECT OF NEURONAL OXIDATIVE STRESS ON THE PATHOPHYSIOLOGY OF BRAIN AND BLOOD BRAIN BARRIER CELLS

Taleeah Allen-Wright, Marta Cherpak, Hyunjo Choi, Peter Fairbanks, Jonathan Huang, Anna Patnaik, Ashwin Reddi, Shradha Sahani, Charlie Urrutia

Directed By:

Dr. Silvia Muro
Associate Professor
Institute for Bioscience & Biotechnology Research
University of Maryland, College Park

ABSTRACT

Neuronal stretching during concussion alters glucose transport and reduces neuronal viability, also affecting other cells in the brain and the Blood Brain Barrier (BBB). Our hypothesis is that oxidative stress (OS) generated in neurons during concussions contributes to this outcome. To validate this, we investigated: (1) whether OS independently causes alterations in brain and BBB cells, namely human neuron-like, neuroblastoma cells (NCs), astrocyte cells (ACs) and brain microvascular endothelial cells (ECs), and (2) whether OS originated in NCs (as in concussion) is responsible for causing the subsequent alterations observed in ACs and ECs. We used H_2O_2 treatment to

mimic OS, validated by examining the resulting reactive oxygen species, and evaluated alterations in cell morphology, expression and localization of the glucose transporter GLUT1, and the overall cell viability. Our results showed that OS, either directly affecting each cell type or originally affecting NCs, caused changes in several morphological parameters (surface area, Feret diameter, circularity, inter-cellular distance), slightly varied GLUT1 expression and lowered the overall cell viability of all NCs, ACs, and ECs. Therefore, we can conclude that oxidative stress, which is known to be generated during concussion, caused alterations in NCs, ACs, and ECs whether independently originated in each cell or when originated in the NCs and could further propagate the ACs and ECs.

CONCUSSION: EXAMINING THE EFFECT OF NEURONAL OXIDATIVE STRESS ON THE PATHOPHYSIOLOGY OF BRAIN AND BLOOD BRAIN BARRIER CELLS

By

Team FORGET IT

Taleeah Allen-Wright, Marta Cherpak, Hyunjo Choi, Peter Fairbanks, Jonathan Huang, Anna Patnaik, Ashwin Reddi, Shradha Sahani, Charlie Urrutia

Thesis submitted to the Faculty of the Gemstone Program of the University of Maryland, College Park, in partial fulfillment of the requirements for the Gemstone Citation 2016

Advisory Committee:
Dr. Silvia Muro (Director)
Dr. Daniel John Dwyer
Dr. Jose Helim Aranda-Espinoza
Dr. Masaaki Torii
Dr. Yu-Chieh Chiu

Acknowledgements

We cannot express enough thanks to the Gemstone Staff for their continued support and encouragement: Dr. Frank Coale, Gemstone Program Director; Dr. Kristan Skendall, Gemstone Associate Director; and Vickie Hill, Assistant Director of Operations, and all the other Gemstone staff. We offer our sincere appreciation for the learning opportunities provided by this program.

We are also grateful to our librarian Ms. Nevenka Zdravkovska, head of the Engineering and Physical Sciences Library, for providing us with resources to use to gather background information for our thesis and for always being available as a resource for our team.

Our utmost gratitude to Dr. Silvia Muro, our mentor, who worked closely with us, conducted our weekly meetings, and supported us throughout our research, to help ensure our success. Without Dr. Muro's continuous support this study would not have been possible.

We would also like to thank members of Muro lab, especially Rachel Manthe who served as our interim mentor, for helping to carry out our research and providing day-to-day assistance inside and outside of the lab. We would also like to thank Krishma Labib, an international student who joined our research team for a semester.

We would like to thank the discussants that served on our panel and provided feedback that helped us perfect and solidify our thesis.

We would also like to thank the ACCIAC Fellows in Innovation and Creativity grant as well as Sigma Xi Grants-in-Aid of Research Program and the Gemstone Program for their supplemental funds, along with those individuals that donated to our Launch UMD page. Without those generous donations and grants from others, portions of this experiment would have not been able to be completed.

List of abbreviations

ACs (Astrocyte Cells)
ATP (Adenosine Triphosphate)
BBB (Blood Brain Barrier)
CNS (Central Nervous System)
DAI (Diffuse Axonal Injury)
DAPI (4',6-diamidino-2-phenylindole)
ECs (Endothelial Cells)
ECL (Enhanced Chemiluminescence)
EDTA (Ethylenediaminetetraacetic acid)
FITC (Fluorescein Isothiocyanate)
GAPDH (Glyceraldehyde-3-Phosphate Dehydrogenase)
GLUT (Glucose Transporter)
NCs (Neuronal Cells)
OS (Oxidative Stress)
PBS (Phosphate-buffered saline)
PFA (Paraformaldehyde)
ROS (Reactive Oxygen Species)
RPMI medium (Roswell Park Memorial Institute medium)

List of Figures

Table Of Contents

CHAPTER 1: OVERVIEW

1.1. Problem Description and Motivation

In the United States alone, an estimated 300,000 sports-related traumatic brain injuries occur each year, showing that concussions are a major concern in today's society [1]. Though there is an understanding of the functional changes in a post concussion state, there is limited understanding of the cellular and molecular level damage that occurs because it cannot be seen on standard imaging tests like CT scans [2].

Concussions are a particularly difficult injury to accurately diagnose and treat because symptoms affect people dissimilarly. One of the difficulties in identifying a concussive injury is that there is an incredibly wide spectrum of signs of injury that are found in patients [3]. The Centers for Disease Control and Prevention cite four main categories into which the indicators are grouped: thinking/remembering (i.e. feeling sluggish and difficulty retaining new information), physical (i.e. headaches and blurry vision), emotional/mood (i.e. irritability, sadness) and changes in sleep patterns [4].

After a concussion is sustained it can lead to bruising and swelling of the brain, tearing of blood vessels and injury to nerves [5]. Though most concussions are mild, if they go untreated or if a second injury is sustained, there can be deadly effects. Because it is difficult to pinpoint the detection of a head injury down to one specific diagnostic method, it is not surprising that a significant portion of cases go undiagnosed every year. In fact, among cases requiring hospitalization, 75%-90% are classified as mildly injured or concussed [6]. This statistic excludes countless instances where head trauma victims were not hospitalized. These challenges in diagnosing any type of brain injury make concussions an especially dangerous form of cranial trauma.

In cases where a concussion is diagnosed there are still gaps in knowledge in terms of the structural changes that occur in the brain. ROS is present in the brain at normal levels, due to ROS playing a signaling feedback role in homeostatic/steady state processes. Once a concussion occurs, the brain responds with an overproduction of reactive oxygen species (ROS), which in turn causes oxidative stress (OS) [7]. OS can have many detrimental effects including cell damage and in some cases cell death [8]; this increase in ROS production impacts homeostasis. ROS plays a role in maintaining homeostasis and for cells to maintain homeostasis, ROS production and consumption must be balanced. The process to balance ROS production and consumption is mediated through the breakdown of glucose via glycolysis [8] When oxidative stress occurs, cells attempt to counteract the oxidant effects and restore the redox balance by activation or silencing of genes encoding defensive enzymes, transcription factors, and structural proteins [9].

Outside of brain chemicals, brain cells are also impacted in the aftermath of a concussion. The concussion causes stretching of neuronal and axonal membranes [6]. This stretching can have cascading effects, which then also create an increase in ROS. After this period, in an effort to reach homeostasis the brain sees a significant increase in the rate at which glucose is metabolized, thus entering a state of hyperglycolysis [10]. Glucose is a very important substrate for energy production in neurons (NCs) [11]. It is transported through the Blood Brain Barrier (BBB), made up of endothelial cells (ECs) [12]. In addition, the BBB is made up of glial cells, such as astrocytes (ACs). Glucose is transported to the brain by BBB and brain cells via the GLUT1 glucose transporter. In the

event of a concussion, glycogen stored in ACs is metabolized into glucose to fuel the NCs.

Though the effects on the brain due to changes in ROS levels and production of OS have been studied, it is unclear how these changes impact ECs, ACs and NCs involved in the BBB and brain tissue post concussion. This study aims to look at how ROS associated with neuronal injury affects ECs and ACs and the overall health of brain and BBB cells, including expression and cellular distribution of GLUT1, cellular morphology and cellular viability.

1.2. Our Approach

Our primary goal was to mimic post-concussive OS in an in-vitro model and examine the effects it has on the BBB and brain cells, specifically ECs, ACs, and NCs. We decided to use hydrogen peroxide (H_2O_2) treatment to induce OS, as prior studies have shown that cellular exposure to H_2O_2 induces OS [7]. Our strategy was pursued in two phases: (1) examining and analyzing the effect of direct extrinsic addition of ROS on ECs, ACs and NCs and (2) examining how OS originally affecting NCs (as in a concussion) would impact ECs and ACs over time. In both of these phases, we examined multiple parameters: ROS levels, cell morphology, expression and localization of GLUT1, and overall cell viability in order to get a holistic view of all the various impacts of OS on each cell type. Upon the completion of phase one, we had baseline data for our parameters to then complete phase two. All of the methods and materials we chose to use in our approach were supported through previous research in this field or repeated experiments before being adopted into our thesis.

1.2.1. Hypothesis

Based on the knowledge described above, we hypothesized that: (a) OS, which is known to be generated during concussion, would cause alterations in each independent cell type of the brain and BBB: NCs, ECs and ACs and (b) the OS originally generated in NCs would further propagate to and affect ECs and ACs. We predicted that the cellular changes that occurred in cells directly exposed to ROS may differ from the changes in cells exposed to NCs in a state of OS, which is important to understand the mechanisms by which concussion affects the brain. In order to verify these hypotheses, we used monocultures vs. co-cultures of brain and BBB cells, to investigate changes due to the presence of OS, generated as a result of ROS production.

1.2.2. Specific Aims

Aim 1 focused on studying if OS causes alterations in the BBB and brain cells, namely NCs, ECs, and ACs, rendering this information as the link between overproduction of free radicals and oxidative damage to molecular, morphological, and viability changes in the brain.

Aim 2 seeks to study if alterations from OS, originating in the NCs, further propagate to the ECs and ACs. OS generated in NCs can cause OS in the other cell types because, in a concussion, the primary cells that are primarily affected are NCs and signaling molecules can be responsible for progressing this damage to the other cell types [12,13].

Whereas Aim 1 looks at individual alterations in the BBB and brain cells, Aim 2 examines the alterations that occur in the ACs and ECs, due to NCs being exposed to ROS and further propagating to these cell types.

1.3. Significance and Innovation

Although concussion research is at the forefront of both scientific and public attention, more research is warranted about the effects of concussion-induced OS at the molecular level. The goal of this study is to view the post-concussive environment in the brain and surrounding areas in order to understand the cellular and molecular effects of a concussion and provide further information on the hallmarks of a concussive injury.

This research is significant because it employs a new *in vitro* model of the BBB and brain cells, that, although used in other contexts, has never been used for concussion-related research. In February 2016, one review article noted that an ideal cell culture model including the BBB was yet to be developed for a concussion [14]. Our research hence is significant because it uses a monoculture model to examine the environment of each individual cell type, then a co-culture model to examine the NCs-ACs and NCs-ECs interactions. Many other *in vitro* models of the BBB have examined the interactions between ECs-pericytes, ECs-glial cells, or primary cultures with one isolated cell type [15]. NCs were first used in an *in vitro* model, replicating the BBB, in 1991 [15]. Not many experiments since 1991 have been done to analyze the interactions of neurons with other cells in the BBB, in the context of concussion [15]. That study demonstrated that it is not necessary for direct contact among endothelial cells and neurons, in order for the induction of occludin expression to occur in endothelial BBB tight junctions [15]. Since the release of these observations, many other studies have opted to use other models such as the ones listed above. Our research is significant because we are using brain and BBB cells within the same co-culture model to mimic the effects on NCs, on the other cell types of the brain and BBB during a human brain concussion.

OS is a damaging pathway involved in all CNS pathologies, infectious,

inflammatory, or degenerative in nature [16]. Our research aligns with other research, demonstrating that OS can be induced simply by injuring cells in culture with specific concentrations of H_2O_2, but our study further studies the consequences of this change on cells distal to those directly injured. With regard to concussion, previous studies have used a model of stretch-induced mechanical injury to injure cells; however, our study used H_2O_2 to injure cells in their *in vitro* model, where H_2O_2 concentration is easily manipulated and controlled.

Lastly, this research is innovative because it looks at the effects of injured NCs on the surrounding cell types, something that is not seen elsewhere in the literature. By looking at all cell types individually; than the cell types simultaneously we were able to note the effects that were caused by the interaction of the cell types. This study adds to the knowledge about the cellular changes that occur in a post-concussed brain. More research in this field needs to be conducted, and our research is contributing in this direction.

CHAPTER 2: BACKGROUND

2.1 Oxidative Stress in the Brain

Throughout the past few decades, free radicals and other reactive small molecules have surfaced as important regulators of many physiological and pathological processes. It is currently known that ROS serves as a signaling messenger to facilitate different biological responses, including programed cell death [17]. On the other hand, it is know that increased levels of these short-lived reactive molecules can employ harmful effects by causing oxidative damage to biological macromolecules and disrupting the cellular

reduction-oxidation (Redox) balance [17]. A disturbance of ROS homeostasis is usually considered as a risk factor for the initiation and progression of diseases and advancement of many harmful side effects to the body. In order to correctly determine if the effects of ROS are beneficial or harmful, it is dependent upon the site, type, and amount of ROS produced, along with the activity of the organism's antioxidant defense system [17].

ROS is generated as a by-product of other biological reactions, such as the mitochondrial election transport chain. Although it is often assumed that mitochondria are the primary source of OS in mammalian cells, there is currently no significant experimental evidence to support this claim [17]. One of the primary ROS species generated, H_2O_2, can readily react to form other ROS species, which are later decomposed to generate other radicals, such as hydroxyl radicals. Recent findings demonstrate that a fraction of mitochondrial H_2O_2, produced by a specialized enzyme as a signaling molecule in the pathway of apoptosis, induces intracellular oxidative stress [18]. It is still unclear, however, whether oxidative stress is the result of a genetic program or the by-product of physiological processes but cells have many enzymatic and non-enzymatic defense mechanisms to counteract oxidative stress in cells [17].

A concussion results in the overproduction of ROS, which in turn hinders the neuronal metabolism and causes OS [7]. OS has multiple harmful effects on the brain at both the cellular and tissue level, making it as important of a treatment issue as the initial impact force of the concussion itself.

OS can cause direct damage to the DNA and is mutagenic. OS may also promote metastasis [16]. Intense OS can cause cell death and, depending on its severity, death of most or all of the cells in a tissue or organ. OS has also been linked to brain aging and

changes in membrane formation, as well as other effects on neurodegenerative diseases [8]. This phenomenon can also be linked to changes in capillary structure and increases in oxidized biomolecules, changes in membrane environments and intracellular calcium storage, and increases release of neurotransmitters [8]. OS is associated with increased production of oxidizing species and associated with a significant decrease in the effectiveness of antioxidant defenses [8].

All forms of life promote a reducing environment within their cells. Enzymes that maintain the reduced state through a constant input of metabolic energy preserve this reducing environment [8]. Disturbances in this normal redox state, which in this case are the concussion-induced OS and aforementioned metabolism malfunction, can cause toxic effects through the production of peroxides and free radicals that damage all components of the cell, including proteins, lipids and DNA [8]. In order to maintain proper cellular homeostasis, a balance must be struck between ROS production and mitigation. Therefore, the introduction of glucose after a concussion replenishes the glucose NCs are rapidly consuming to restore their chemical imbalances, possibly decreasing the overproduction of ROS.

Concussion induced OS also leads to the shifting of neuronal glucose metabolism from oxidative phosphorylation to glycolysis via alterations to mitochondrial mechanisms, as described below.

2.2 Metabolic Effects of Concussions

Glucose is considered to be the main substrate for energy usage in NCs [11]. This is achieved by performing cellular respiration, consisting of glycolysis and oxidative

phosphorylation, in order to create energy in the form of adenosine triphosphate (ATP) [11]. ATP is then used to power a wide variety of cellular processes. Studies using fluorescently labeled glucose molecules have proven that the majority of these processes occur in NCs, with ACs (a type of neuron-supporting glial cell) contributing a small amount of ATP through oxidative phosphorylation [11]. Characteristics of enzymes active during glycolysis and thermodynamic considerations point towards glucose as the main energy source for NCs [19]. Glucose also passes through the BBB much more readily than other possible energy substrates, such as lactate [19].

A concussion occurs when the brain experiences a mechanical "shake" as a result of quick acceleration caused by a force [6]. This stretching causes the membrane to let calcium and sodium ions through, disrupting the concentration gradient and causing NCs to send temporally and spatially abnormal electrical impulses [10]. Consequently, high quantities of excitatory amino acid neurotransmitters are released into the synapse [10]. In an effort to restore the membrane potential, the sodium-potassium pumps on the membrane of NCs begin to work at an increased level, triggering an increased need for ATP [20]. Because glucose is necessary for cells to perform cellular respiration for ATP, immediately following a concussion the brain goes through a period of high glucose usage, or hypermetabolism [20]. Therefore, the rate of glycolysis is heavily increased in order to generate additional ATP to meet the increased energy demand [20].

This increased neuronal demand for glucose is difficult for the cell to meet because OS causes NCs to shift from oxidative phosphorylation to anaerobic glycolysis. Axonal depolarization causes an increase in intracellular calcium. Mitochondrial calcium overload leads to an increase in ROS [21]. Experiments show that ROS localize in the

mitochondrial membrane and their presence compromises the electron transport chain, located in the mitochondrial membrane [6]. This reinforces the shift from oxidative phosphorylation to glycolysis and leads to difficulty in meeting the higher energy demand caused by concussion [21].

The presence of ROS in the mitochondria disrupts the sodium and potassium ionic balance, causing neuronal depolarization and leading to an increase in energy needed for the sodium-potassium pump to return the membrane potential to resting state [6]. However, with the presence of ROS in the mitochondria, oxidoreductive reactions are impaired and the mitochondria cannot maintain the correct phosphorylating capacity in order to convert ADP to ATP [6]. Since the neuronal production of ATP by oxidative phosphorylation is hindered by ROS, the cell resorts to producing energy via oxygen-independent glycolysis [6]. The NCs greatly increase glucose consumption after a concussion, but because glycolysis is exclusively used, less ATP is generated per glucose molecule than in the healthy NCs [6].

The brain enters a state of hyperglycolysis [10]. During the first thirty minutes following a traumatic brain injury, the rate of glucose breakdown increases up to 46% from normal levels. However, during the next five hours after a concussion, as the cellular glucose levels are depleted, glucose metabolism slows to nearly half the normal rate. [10]. The consequent glucose hypometabolism can last up to five days, but severe trauma can have lingering effects for months [10].

An overproduction of ROS also results in lipid peroxidation, which is the breakdown of lipids through oxidation. Lipids form the membrane of cells; therefore, ROS can be extremely damaging to cells as their membranes become degraded,

sometimes beyond repair. This process starts around one minute after the initial trauma and continues for one to two days afterwards [6]. Thus, NCs must rely further on less efficient anaerobic glycolysis, which compounds into an overall energy deficit, potentially causing major consequences to the brain [10].

2.3 Transport of Glucose Across the Blood-Brain Barrier

The BBB is the interface between the circulatory and the central nervous systems (CNS) that prevents the entry of potentially harmful and unwanted substances into the brain [22]. The BBB is composed ECs with tight junctions, separating the CNS from the bloodstream, and subjacent ACs. The transport of certain fluids, macromolecules, and blood cells occurs across this barrier; however, the BBB carefully regulates what substances are allowed to pass through the capillaries into the brain [12].

Transport across the BBB is regulated by interactions between the ECs, ACs and also pericytes [12]. Molecules can move through the barrier by a number of ways, depending on size and polarity. The diffusion rate of these molecules also depends on their lipid solubility [23]. Small water-soluble molecules, like H_2O_2, are able to move through the tight junctions formed by the ECs, whereas lipid-soluble molecules can diffuse through the EC membrane [23]. Larger molecules can be moved into the abluminal side through receptor-based or absorptive transcytosis [23]. Also, transport proteins or carriers are needed to transport nutrients such as amino acids and glucose into the brain [23].

Glucose travels through the bloodstream in order to reach cells to satisfy their energy requirement; glucose transporters facilitate the transport of glucose into the body's cells [24]. Glucose is transported by the GLUT transporter proteins, which consist

of 12 membrane-spanning domains and an N-linked glycosylated site in the extracellular domain of this molecule. GLUT1 is the primary transporter of glucose in ACs and on the membrane of the ECs [24].

Once glucose is transported into the EC cytoplasm and has moved closer to the abluminal side, the molecule is processed by enzymes and can be transported into the ACs for storage or from ACs to NCs for energy usage. ACs store glucose in the form of glycogen [25]. During periods of intense neural activity, like during a concussion, the glycogen is broken down into glucose, which then moves out of the ACs via GLUT1 and is taken up by NCs [26]. There is not much known about how the expression and localization of GLUT1 changes in the cells that comprise the BBB as a response to neuronal OS, as well as the overall morphology and viability of these cells due to OS.

CHAPTER 3: MATERIALS AND METHODS

3.1 Antibodies and Reagents

Monoclonal mouse anti-human GLUT1 was clone A4 (Santa Cruz Biotechnology; Dallas, TX). Polyclonal rabbit anti-human Glyceraldehyde-3-Phosphate Dehydrogenase (GAPDH) was clone FL-335 (Santa Cruz Biotechnology). FITC goat anti-mouse IgG was used as a secondary antibody (GE Life Sciences; Buckinghamshire, UK). Tris-HCl Gels (Bio-Rad; Hercules, CA), RIPA buffer (Thermofisher; Waltham, MA), enhanced chemiluminescence (ECL) Western Blotting Detection Reagent (GE Life Sciences; Buckinghamshire, UK), and Bradford Reagent (Bio-Rad). CellRox® Green Reagent and Live/Dead Viability Kit was from Life Technologies (Carlsbad, CA).

3.2 Cell Culture Propagation

Three human cell types were used in this study: human brain microvascular ECs (Applied Cell Biology Research Institute; Kirkland, WA), ACs (Lonza Walkersville, Inc; Walkersville, MD), BE(2)-C NCs derived from a neuroblastoma (ATCC, Manassas, VA). All three cell types were cultured at 37°C, 5% CO_2, and 95% humidity.

ECs were propagated in culture flasks coated with 1% gelatin, in media consisting of Gibco® Roswell Park Memorial Institute medium (RPMI) 1640 (Cellgro, Manassas, VA), 20% fetal bovine serum (Cellgro, Manassas, VA), 2 mM glutamine, 100 μg/mL penicillin, 100 μg/mL streptomycin, 100 μg/mL heparin and 30μg/mL endothelial growth supplement [27]. ACs were propagated in flasks coated with 1% gelatin, in media consisting of Gibco® RPMI 1640, 15% fetal bovine serum, 2 mM glutamine, 100 μg/mL penicillin, 100 μg/mL streptomycin, and 50 μg/mL gentamicin [27]. NCs were propagated in flasks coated with 1% Matrigel® (Corning, Tewksbury, MA) in culture media consisting of Gibco® RPMI 1640, 10% fetal bovine serum, 2 mM glutamine, 100 μg/mL penicillin and 100 μg/mL streptomycin, and 100 μg/mL sodium pyruvate [28]. Once grown to confluency, the cells were passaged twice until there were seven generations. Following that passage they were cryopreserved in Cell Freezing Media (Thermofisher; Waltham, MA) and frozen in liquid nitrogen until thawed for use.

3.2.1 Monoculture Model

To study the effects of OS on cells relevant to the BBB and brain, ECs, ACs, and NCs were individually thawed in their respective culture medias. ECs were seeded at a density of 10^5 cells/cm^2 onto 1% gelatin-coated glass coverslips placed in culture plates in culture media described above [27]. ACs were seeded at a density of $5x10^4$ cells/cm^2 onto

1% gelatin-coated glass coverslips in culture plates [27]. NCs were seeded at a density of 10^4 cells/cm^2 on 1% Matrigel®-coated glass coverslips in culture plates. The media in the culture plates was changed the day following seeding and the cells were allowed to grow for 24 hours. For experiments, cells were then placed in the "healthy" (control) or "injured" condition. The healthy condition consisted of changing the media and incubation for 15 minutes at 37°C. The injury consisted of treating each cell type with 0.5 mM or 5 mM H_2O_2 for 15 minutes at 37°C. This culture model is shown in Figure 1A (see section 3.2.2).

3.2.2 Transwell Model

To study the effect of neuronal OS on the other cells, a Transwell insert (Figure 1B), was used to create a co-culture of NCs with the cells involved in the BBB [29], either ECs and ACs. First, either ECs or ACs were grown to confluence on the apical side of the 0.4 μm pore transwell insert (Fisher Scientific; Waltham, MA) in their respective culture medias without the presence of NCs. ECs were seeded at a density of $1.5x10^5$ cells/cm^2 and ACs were seeded at a density of $7.5x10^4$ cells/cm^2 without any coating on the Transwell membrane. NCs were seeded independently at a density of 10^4 cells/cm^2 on 1% Matrigel®-coated glass coverslips in culture plates. NCs were then treated under either "healthy" (control) or "injured" (H_2O_2) conditions, as described in 3.2.1. Then NCs were washed with PBS to eliminate residual H_2O_2 and the ECs or ACs on the Transwell inserts were placed in co-culture with control or injured NCs for a period of 5 hours or 24 hours. After this, different parameters were tested blind to the control versus injury.

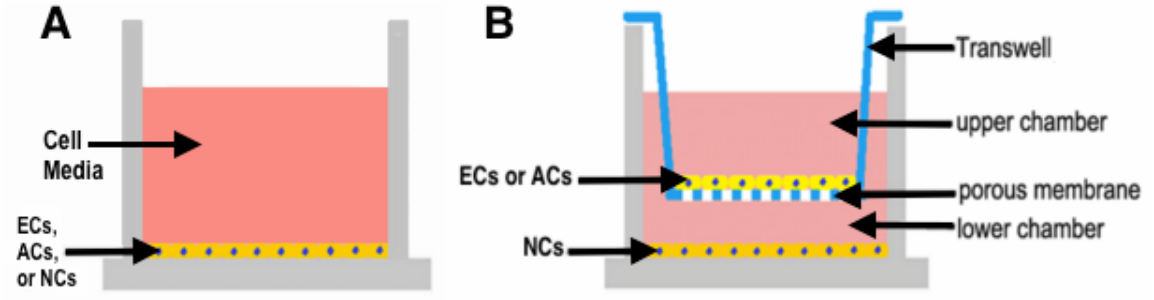

Figure 1. (A) Diagram of our cell monoculture model. (B) Diagram of our transwell biculture model [30].

3.3 Reactive Oxygen Species (ROS)

ROS was used to verify the OS levels experienced in cells after H_2O_2 injury. For this purpose, CellROX® Green Reagent assay (Life Technologies; Eugene, Oregon), a fluorogenic probe for measuring OS in live cells was used [31]. First, ECs, ACs, and NCs were treated with varying concentrations of H_2O_2 (0 mM- 5mM) and incubated for 15 minutes at 37°C. The cells were then washed three times with RPMI and incubated for 30 minutes at 37°C with 5 µM CellROX® dye. The cells were subsequently washed three times with RPMI, fixed with 2% paraformaldehyde (PFA) for 15 minutes at room temperature, and imaged at 60X magnification using a filter compatible with fluorescein isothiocyanate excitation (FITC) [32] and a fluorescence microscope (see description of settings in section 3.8). In order to define the cell area, phase contrast images were used, as well as the outline of the fluorescence as a guide. In the transwell model, the fluorescence alone was enough of an indicator to note the border of a cell. Images were then used to calculate the mean and sum fluorescence intensities of the cells, and background regions (a control subtracted from cell measurements) using ImagePro (Media Cybernetics, Inc., Rockville, MD, USA) at 60X magnification.

For detailed ROS Monocellular Model Procedures, see Appendix Sections A.

3.4 Morphology

Morphological parameters were used to analyze the changes in shape of injured versus control ECs, ACs, and NCs in the monoculture and Transwell models. Cells were injured with varying concentrations (from 0 mM to 5 mM) of H_2O_2 for 15 minutes. Cells were then washed with RPMI and fixed with 4% PFA in phosphate buffer saline (PBS) for 15 minutes. Cells were then washed and mounted onto slides with mowiol (Sigma-Aldrich Co., St. Louis, MO, USA). Cell microscopy was conducted and images were used to quantify the relative effects of the H_2O_2 treatment on the overall morphology of the three cell types. For this purpose, cells were examined via phase contrast microscopy at 60x magnification for the monocellular model. In the co-culture model, a Texas Red filter (60x) was used to improve visibility due to the presence of the Transwell membrane. Following that, images were filtered using the program ImagePro (Media Cybernetics, Inc., Rockville, MD, USA). ImageJ's (National Institutes of Health, Bethesda, MD, USA) image analysis feature was then used to trace around the perimeter of each cell. Following this, several parameters were quantified for comparison:

(A) Overall 2-dimensional cell area, which is measured as the space within the traced cell perimeter, quantified in μm^2;

(B) Circularity, which measures a cell's roundness relative to a perfect circle, given by the formula $C = 4\pi (A/p^2)$, where A represents cell area and p represents the perimeter. This parameter ranges from 0 to 1; measurements close to 0 indicate a more oblong or non-circular shape while measurements closer to 1 indicate higher roundness.

Circularity is a unitless measurement that represents the ratio of the area to the perimeter, since $A = \pi r^2$ and perimeter of a circle = $2 \pi r$ then $4(\pi r^2/(2 \pi r)^2)$ equals one;

(C) Feret diameter, which is the measurement between the two furthest ends of a cell, equivalent to the longest distance between two ends and indicative of cell elongation.

(D) Gap distance between cells, defined as the largest quantifiable distance between the edges of any two nearby cells

For detailed Morphology Monocellular and Transwell Model Procedures, see Appendix sections B and C, respectively.

3.5 Western Blot

This assay was used to assess the relative expression of GLUT1 (Pardridge, Boado, and Farrell, 1990). Cells were first rinsed with PBS at 37°C and then incubated with 5mM H_2O_2 for 30 minutes. Cells were then rinsed again using PBS at 37 ° C and lysed using RIPA buffer (ThermoFisher Scientific, 25mM Tris HCl pH 7.6, 1% NP-40, 1% sodium deoxycholate, 0.1% SDS) with a 0.005 mM Ethylenediaminetetraacetic acid (EDTA) solution. A Bradford assay was conducted and measured at a wavelength of 595 nm. A standard curve using Bovine Serum Albumin (BSA) was used to determine the concentration of protein in each lysate. Then, a 4-15% polyacrylamide gel was loaded with a total of 20 µg of protein from the cell lysate. SDS-PAGE electrophoresis was conducted at 80V/25mA for 1.5 hours. The protein was then transferred to a nitrocellulose membrane using a transfer buffer (2.5 mM Tris, 19.2 mM glycine, 0.01% SDS, 20% methanol). The membrane was then blocked with 5% nonfat milk in 1 mM Tween-20 PBS (PBS-T) for 1 hour, and incubated overnight at 4°C with 1 µg/mL

monoclonal mouse anti-human GLUT1 and 1 μg/mL polyclonal rabbit anti-human GAPDH in in 3% nonfat milk in PBS-T. GAPDH is a ubiquitous protein in injured and control cells and it was used as a loading control to normalize GLUT1 signal .

After incubation with the primary antibodies, the membrane was washed with PBS-T a total of six times (for five minutes per wash) and incubated for 70 minutes at room temperature with 0.03 μg/μL HRP-conjugated goat anti-mouse IgG and 0.1 μg/μL goat anti-rabbit IgG (GE Life Sciences; Pittsburgh, PA, USA) in 3% nonfat milk in PBS-T. Protein band detection was then conducted by chemiluminescence by placing ECL solution (Amersham Plus, GE Life Sciences; Pittsburgh, PA, USA) on the membrane for 5 minutes, followed by exposing it in a dark room for 1.5 minutes using Kodak X-ray biofilm single side emulsion paper. Densitometry, the quantitative analysis of GLUT1 and GAPDH band density, was used to analyze the relative density of the bands via the ImageJ software (National Institutes of Health, Bethesda, MD, USA). GLUT1 density was normalized to the density of the housekeeping protein, GAPDH, by calculating the GLUT1/GAPDH band ratio. The GLUT1/GAPDH ratio of the injured cells was compared to that of the control condition, by calculating it as a percent relative to the control.

For detailed Monocellular Western Blot Procedure, see Appendix Section D.

3.6 Localization of GLUT1

Fluorescence microscopy was utilized to determine changes in the overall expression and subcellular localization of GLUT1 in cells. Both the injured and control cells were fixed with 2% PFA for 15 minutes at 37 °C, and permeabilized with 0.2% Triton X-100 then incubated overnight at 4°C with 1 μg/mL mouse anti-human GLUT1

in PBS. All cells were then washed with PBS and incubated for 1 hour at room temperature with 1μg/mL FITC-conjugated goat anti-mouse secondary antibody (GE Life Sciences; Buckinghamshire, UK) in PBS and stained with DAPI. Then the samples were mounted on slides for imaging using mowiol.

Imaging was conducted at 60X magnification using phase contrast and the FITC blue and 4',6-diamidino-2-phenylindole (DAPI) channels. To quantify GLUT1 levels, the mean and sum intensities of the fluorescence of each cell were recorded and analyzed using ImagePro Analyzer software (Media Cybernetics, Inc; Rockville, MD, USA). Intensities were recorded from the entire area of the cell, as well as just the perinuclear region (the nucleus of the cell and ≈2 μm of the cytoplasmic region surrounding it as identified by the DAPI staining) in order to account for differential distribution of GLUT1 in this area.

For detailed Localization Monocellular and Transwell Model Procedure see Appendix Section E and F, respectively.

3.7 Cell Viability

Cell viability experiments were performed to determine the ultimate effects of OS. Control and H_2O_2-treated cells were stained using the Live/Dead Viability/Cytotoxicity kit for mammalian cells (Life Technologies; Eugene, Oregon). This uses the fluorescent dyes calcein AM at 0.1 μM (green) and ethidium homodimer at 1 μM (red) to stain live and dead cells, respectively. The cells were then washed and fixed for 15 minutes at room temperature with 4% PFA. The samples were then imaged on ImagePro (Media Cybernetics, Inc, Rockville, MD, USA) with a fluorescence

microscope using the green and red filters at 10X magnification. The cells on each slide were examined on ImagePro (Media Cybernetics, Inc, Rockville, MD, USA) and then the live (green) and dead (red) cells in each image were manually counted to compare between control and injury conditions. When grown in co-culture, the cells were trypsinized from the Transwell membrane and stained using trypan blue (Sigma-Aldrich Co., St. Louis, MO, USA). The cells were then examined using a light microscope at 10X magnification. The number of live (no stain) and dead (blue) cells were manually counted on a hemocytometer.

For detailed Cell Viability Monocellular and Transwell Model Procedure see Appendix Section G and H, respectively.

3.8 Microscopy

All the imaging described in the methods above was conducted using an Olympus IX81 microscope (Olympus, Inc., Center Valley, PA) equipped with an ORCA-ER camera (Hamamatsu, Bridgewater, New Jersey), 10x or 60x objective (Olympus Uplan FLN; Olympus) and DAPI, FITC, and Texas-Red filters (1160A-OMF, 3540B-OMF, 4040B-OMF; Semrock, Inc., Rochester, NY). Slidebook 4.2 (Intelligent Imaging Innovations, Denver, Colorado) was used to collect the images, which were then analyzed using either Image-Pro (Media Cybernetics, Inc; Rockville, MD, USA) or ImageJ (National Institutes of Health, Bethesda, MD, USA).

3.9 Statistical Analysis

A Student's t-test was used for the analysis of this data with statistical significance at a p-value less than 0.05. Each experiment was conducted with 3-5 independent trials with each trial consisting of 2 independent wells per condition. For analysis, 10 randomly selected cells per well for a total of 60 cells per condition were imaged and analyzed.

CHAPTER 4: RESULTS AND DISCUSSION

4.1 Selection of Injury Model

As per our first aim, our goal was to identify how OS, which is known to be generated in concussions, individually affects BBB and brain cells. For this purpose, we sought to use an injury model that would mimic OS. This was achieved by individually treating the NCs, ECs, and ACs with 0.5 mM H_2O_2 or 5 mM H_2O_2. These two concentrations of H_2O_2 were selected based on a study done to examine the effects that H_2O_2 had on porcine aortic ECs [33]. After treating cells, they were labeled with CellROX® green dye and images of the cells were taken by fluorescence microscopy. This dye is naturally weakly fluorescent; however, upon oxidation by ROS, the dye displays a bright green fluorescence. This reagent allowed us to measure oxidative stress in live cells and it was compatible with traditional fluorescence microscopy so it was an appropriate dye for our experimentation [31].

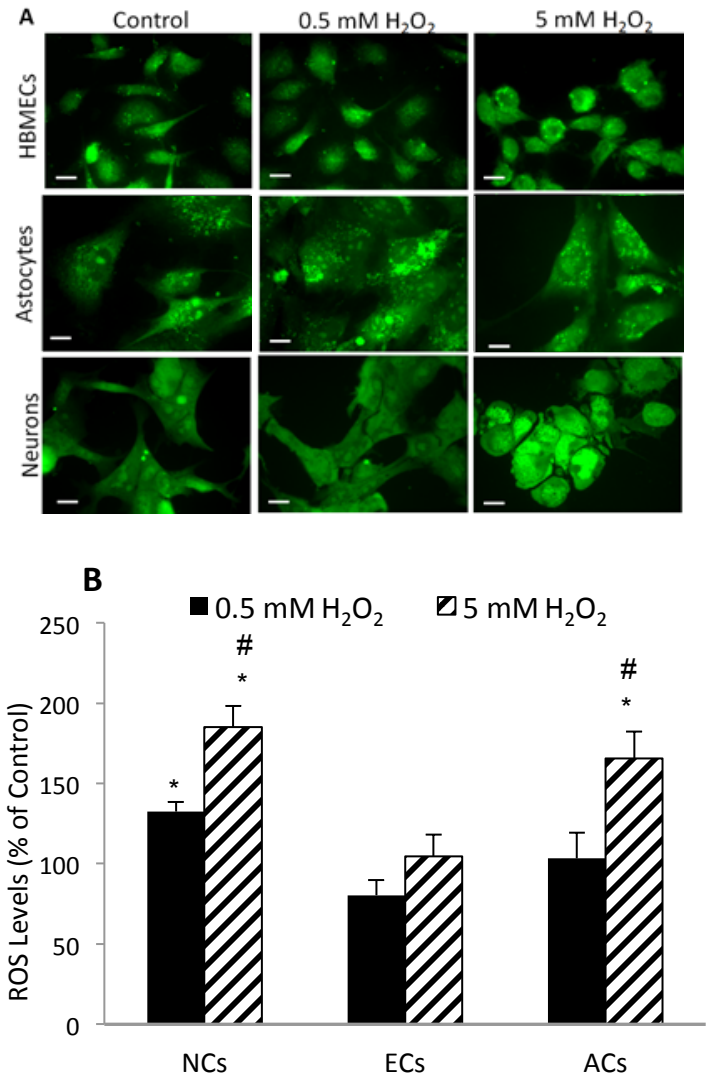

Figure 2. Effect of H_2O_2 on ROS production. (A) Cells were labeled with CellROX® green dye after a 15 minute treatment under control, 0.5 mM H_2O_2, and a 5 mM H_2O_2 conditions. Images of NCs, ECs, and ACs were taken by fluorescence microscopy at 60x magnification. Scale bars = 10 μm. (B) Quantification of ROS levels in (A) using mean intensity to determine ROS levels produced as a result of H_2O_2 injury as compared to control. Data are mean ± SEM. *, Compares H_2O_2 injury to control; $p < 0.05$ by student's *t*-test. #, Compares 0.5mM to 5mM H_2O_2 injury.

As seen in microscopy images shown in Figure 2, and then quantification shown in Figure 2B, a 5 mM H_2O_2 treatment led to increased ROS levels in all cells, when

compared to the 0.5 mM H_2O_2 treatment. In the NCs experiments, the 0.5 mM H_2O_2 were 132.5% of control and the 5 mM H_2O_2 were 184.9% of the control (Figure 2B). Although in the EC experiments, no increase in ROS levels was observed when treated with 0.5 mM H_2O_2, there was a very slight increase, 104.6% of control, when treated with 5 mM H_2O_2, although not statistically significant. The ACs treated with 0.5 mM H_2O_2 experienced an non-significant increase of 103.3% of control in ROS levels and the ACs treated with 5 mM H_2O_2 a 165.5% of control in ROS levels. Thus we can see there is a dose-dependent increase in ROS levels for all cell types.

In all three cell types the highest increase in ROS levels was observed when treated with 5 mM H_2O_2, verifying the efficacy of H_2O_2 treatment in producing ROS in NCs, ECs, and ACs. These results are consistent with the findings in prior research, which states that high pathological levels of H_2O_2 result in OS and apoptosis [34]. From the three cell types, NCs experienced the highest levels of ROS after an H_2O_2 injury. A potential explanation for why the NCs experienced higher ROS levels is that the basal level of ROS is higher in NCs due to a higher metabolism. Then, during an H_2O_2 injury, the synergy of ROS produced in normal conditions in addition to the ROS due to injury is higher than the ROS levels in ECs and ACs.

4.2 Effect of ROS Injury on Cell Morphology

After selecting a method for adding exogenous H_2O_2 to the BBB and brain cells, we focused on observing and quantifying the effects ROS would have on the overall morphology of the cells. Investigating changes in morphology allows us to look at visible characteristics of the cell, where we can quantify the differences in physical appearance

that are the most obvious between test conditions. Therefore, we chose several dimensional parameters to see if there were any holistic differences in the appearance of the cells after induction of ROS. To quantify morphology we examined cell area, cell circularity, gap between adjacent cells, and feret diameter. Measuring the distance between cells is an indication of how confluent the cells in the sample are and quantifying feret diameter, the length of the longest side of the cell, is an indication of how much the cells are stretching after experiencing an H_2O_2 injury. Figures 3, 4, and 5 all show that H_2O_2 injury result in gross level morphological effects on NCs, ECs, and ACs.

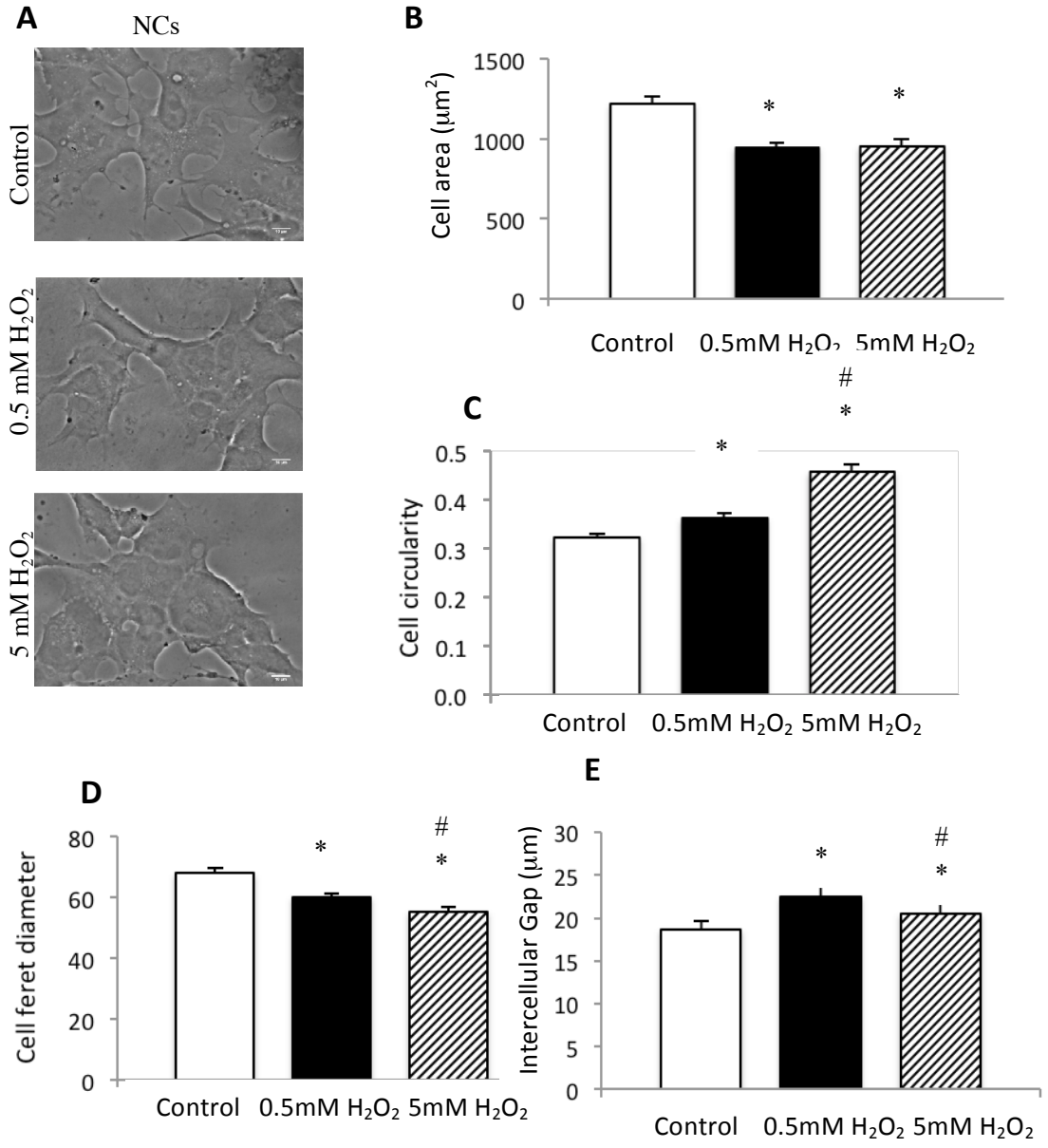

Figure 3. Effect of ROS on NC morphology. (A) Experimentation involved cell incubation with control, 0.5 mM H_2O_2, and a 5 mM H_2O_2 solution for 15 minutes. Images of ACs were then taken by phase contrast microscopy at 60x magnification. Scale bars = 10 μm. The following parameters were quantified from images: (B) Cell area of ACs. (C) Circularity. (D) Cell feret diameter. (E) Gap between ACs. * Compares H_2O_2 injury to control; # compares 0.5mM to 5mM H_2O_2 injury. Data are mean ± SEM.

Figure 3A shows the images taken of the NCs. Figure 3B shows no statistically significant difference between total cell surface area between 0.5 mM H_2O_2 injury and 5 mM H_2O_2 injury; however, both concentrations cause a noticeable change from the control. Also, a 5 mM H_2O_2 injury causes a significant increase to 142.1% of control in cell circularity (Figure 3C). Figures 3D and 3E show that both H_2O_2 concentrations similarly decrease and increase Feret diameter and cell gap distance, respectively.

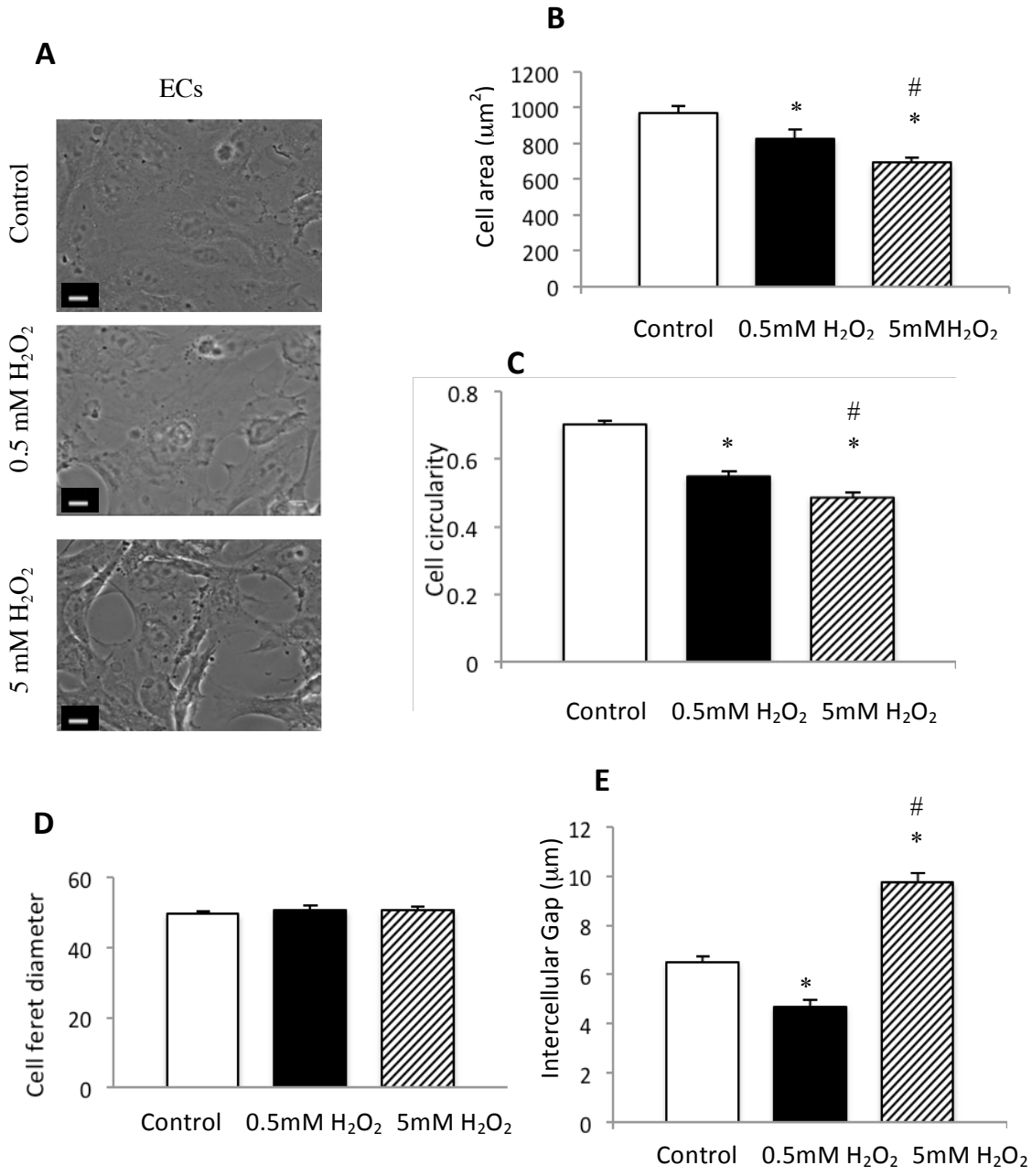

Figure 4. Effect of ROS on EC morphology. (A) Experimentation involved cell incubation with control, 0.5 mM H_2O_2, and a 5 mM H_2O_2 solution for 15 minutes. Images of ACs were then taken by phase contrast microscopy at 60x magnification. Scale bars = 10 μm. The following parameters were quantified from images: (B) Cell area of ACs. (C) Circularity. (D) Cell feret diameter. (E) Gap between ACs. * Compares H_2O_2 injury to control; # compares 0.5mM to 5mM H_2O_2 injury. Data are mean ± SEM.

Figure 4A shows the images taken of ECs. Figure 4B shows that a 5 mM H_2O_2 injury causes a 13.6% larger reduction in cell area than a 0.5 mM H_2O_2 injury. Additionally, a 5 mM H_2O_2 injury causes a greater change in cell circularity between the two H_2O_2 concentrations relative to the control. There was no statistically significant difference in the Feret diameter between the control and injury groups (Figure 4D). The cells treated with 0.5 mM H_2O_2 have an average intercellular gap 72.3% of the control, while the cells treated with 5mM H_2O_2 have a gap 150.6% of the control. The result of the cells treated with 5 mM H_2O_2 supports our finding that cell gap increases with H_2O_2 injury.

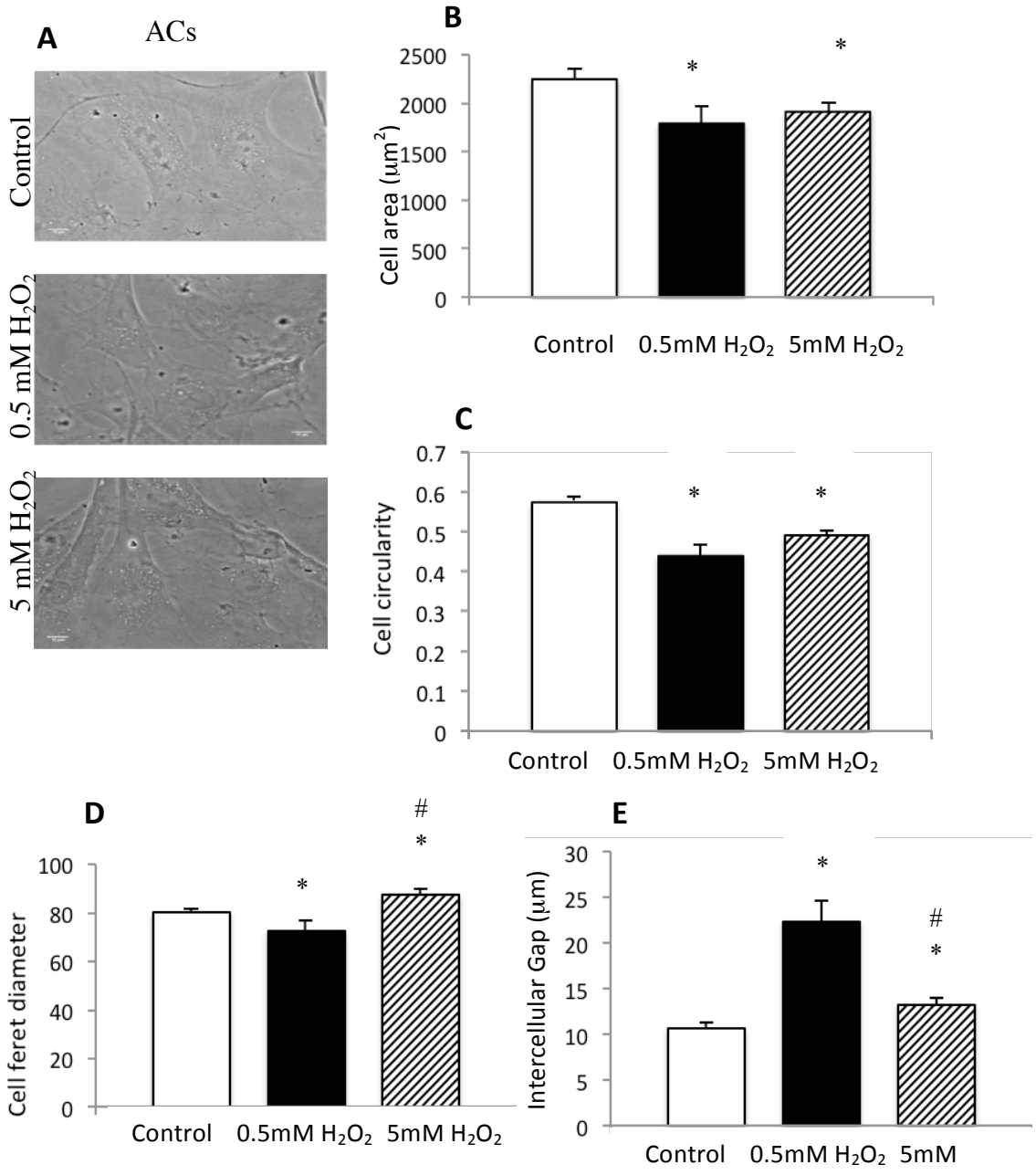

Figure 5. Effect of ROS on AC morphology. (A) Experimentation involved cell incubation with control, 0.5 mM H_2O_2, and a 5 mM H_2O_2 solution for 15 minutes. Images of ACs were then taken by phase contrast microscopy at 60x magnification. Scale bars = 10 μm. The following parameters were quantified from images: (B) Cell area of ACs. (C) Circularity. (D) Cell feret diameter. (E) Gap between ACs. * Compares H_2O_2 injury to control; # compares 0.5mM to 5mM H_2O_2 injury. Data are mean ± SEM.

Figure 5A shows images taken of ACs. Figure 5B shows that there was no statistically significant difference in the cell area between the two H_2O_2 concentrations, though they both decreased significantly from the control. The 0.5 mM H_2O_2 injury yielded a slightly larger decrease in cell circularity (Figure 5C). Figures 5D and 5E shows that the cells treated with 0.5 mM H_2O_2 showed both the largest intercellular gap and the smallest Feret diameter. Smaller overall Feret diameters indicate smaller and less confluent cells, reflected by the increase in the gap between the cells.

These morphological changes depict gross level effects on all three cell types when exposed to H_2O_2 injury. Our findings show that when treated with 5 mM H_2O_2 cell gap increases in NCs, ECs, and ACs and cell area decreases. In addition, Feret diameter decreases in ECs and NCs. Overall, the cells treated with 5 mM H_2O_2 showed more consistent morphological trends than the cells treated with 0.5 mM H_2O_2, which suggests that this higher H_2O_2 concentration may be a more suitable model to induce and track an injury to the cells.

4.3 Effect of ROS Injury on GLUT1 Expression

We observed gross level changes in the cells' physical appearance, however these gross changes did not indicate changes in metabolism, specifically in glucose transport and use. Therefore, we sought to then focus specifically the GLUT1 glucose transporter, and examine whether its expression changed upon cell exposure to ROS. Western blot was used to analyze the effect of H_2O_2 on expression of GLUT1, 30 minutes after cell injury, with either 0.5 or 5 mM H_2O_2. GLUT1 expression was quantified by the ratio of GLUT1/GAPDH band density, normalized relative to the control condition.

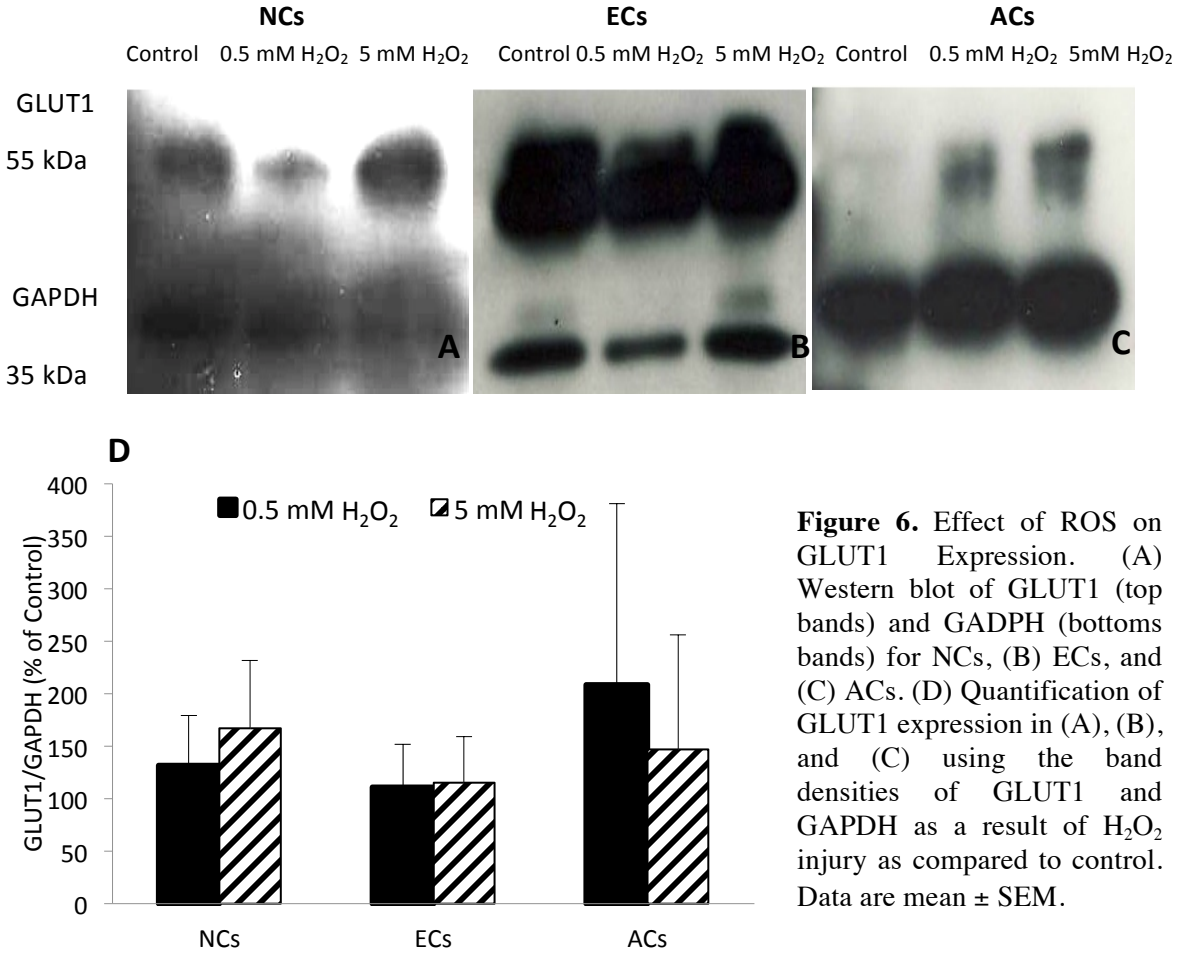

Figure 6. Effect of ROS on GLUT1 Expression. (A) Western blot of GLUT1 (top bands) and GADPH (bottoms bands) for NCs, (B) ECs, and (C) ACs. (D) Quantification of GLUT1 expression in (A), (B), and (C) using the band densities of GLUT1 and GAPDH as a result of H_2O_2 injury as compared to control. Data are mean ± SEM.

Western blot of H_2O_2 treated NCs revealed that the expression of GLUT1 increased with higher doses of H_2O_2 introduced to the cells. GLUT1 expression in the 0.5 mM condition increased to 131.8% of the control, and the 5 mM condition increased to 161.1% of the control (Figure 6A). However, the results did not show any statistical significance, due to large amounts of variability between trials. H_2O_2 treated ECs showed a similar, albeit generally less steep dose-dependent effect. GLUT1 expression rose to 110.9% of the control in the 0.5 mM condition, and to 115.1% of the control in the 5 mM

condition (Figure 6B). However, as seen in the NCs, results were not statistically significant.

ACs also revealed an increase in GLUT1 expression with H_2O_2 treatment; although the results were inverted from that of NCs and ECs. ACs GLUT1 expression rose to 208.8% of the control in the 0.5 mM condition, but only rose to 147.1% of the control in the 5 mM condition (Figure 6C). It is possible that GLUT1 expression peaks at lower levels of H_2O_2 and declines at higher levels, as seen in the 0.5 mM condition having denser bands than the 5 mM condition, although this seems unlikely given that there is no precedent in the literature, or even amongst NCs and ECs, for this type of trend. On the other hand, it is more likely that these inverted results can be attributed to the extraordinarily high levels of variability between trials. The variability found in the ACs expression was markedly higher than that of NCs and ECs trials. As with NCs and ECs, there was too much variability between individual trials to deem these results statistically significant.

Because the variability between trials for all three cell types rendered western blot data non-significant, it was hypothesized that changes in GLUT1 expression may be better tested evident by examining the distribution of the transporter within the cell.

4.4 Effect of Direct ROS Injury on GLUT1 Cellular Localization

To determine the distribution of GLUT1, it was necessary to visualize protein expression within the cells themselves. Fluorescence microscopy was utilized to further investigate the effect of a 5mM H_2O_2 injury on GLUT1 expression 15 minutes after treatment. Because we observed an H_2O_2 dose-dependent increase in ROS levels, as well as in GLUT1 expression via western blot (barring the AC trials that displayed high variability),

we decided to focus solely on the 5mM H_2O_2 concentration in order to induce larger, more observable changes in our subsequent experiments. Cells underwent immunostaining with a GLUT1 mouse anti-human antibody, followed by a FITC-conjugated goat-anti-mouse antibody (Figure 7A).

Figure 7. Effect of ROS on GLUT1 cellular localization. (A) Experimentation included a control and 5 mM H_2O_2 injury for 15 minutes. Afterwards, GLUT1 was immunostained using a primary and FITC-secondary antibody, and images of NCs, ECs, and ACs were taken by fluorescence microscopy on the FITC and DAPI (nucleus) channels at 60x magnification. FITC staining achieves the green color, representing GLUT1 expression and the blue color represents cell nuclei. Scale bars = 10 μm. (B) Whole cell mean and sum intensity of fluorescence in injured cells as a percentage of intensities in control cells. (C) Perinuclear region mean and sum intensity of fluorescence in injured cells as a percentage of intensities in control cells. (D) Sum intensity of fluorescence in the perinuclear region expressed as a percentage of the whole cell sum intensity. Data are mean ± SEM. *, Compares 5mM H_2O_2 injury to control. $^{\#}$, Compares ACs to ECs; $p < 0.05$ by student's *t*-test.

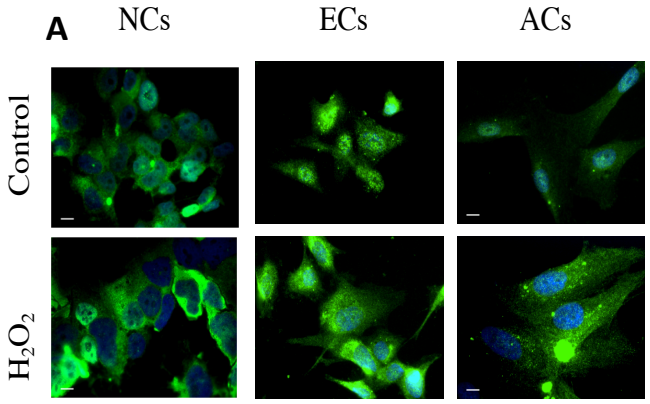

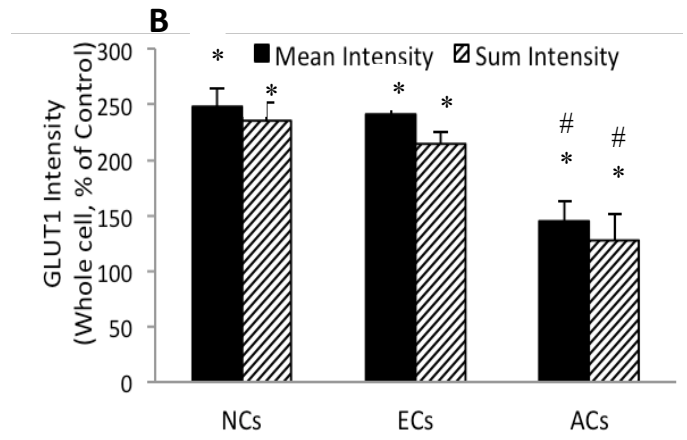

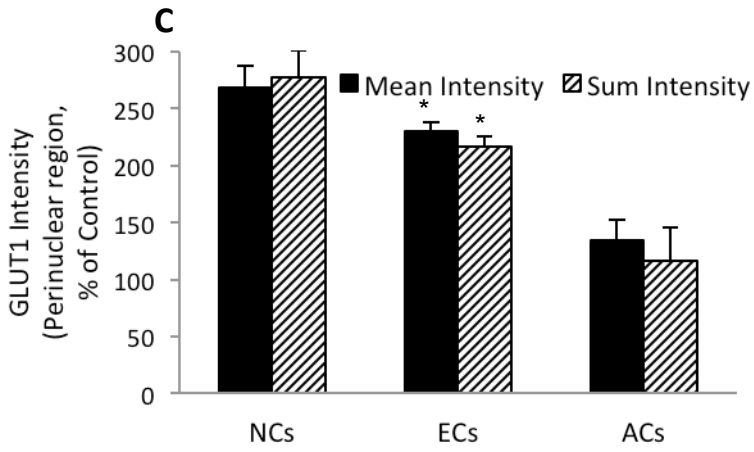

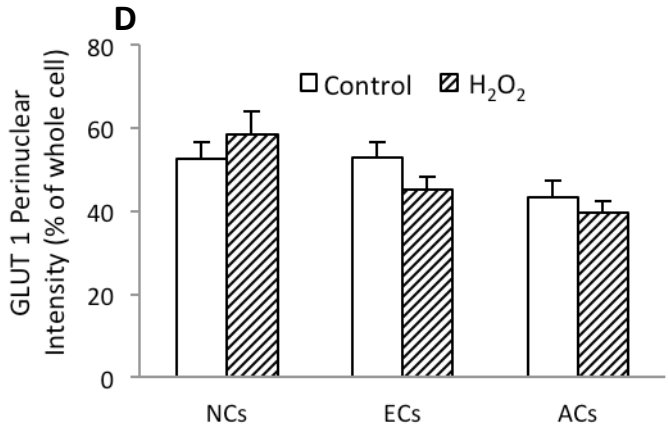

The mean (expression per unit area) and sum (total expression) intensities of the GLUT1 fluorescence were then measured and normalized relative to the control condition. First, the fluorescent intensities were taken from the entire cell area, in order to

identify overall cellular changes in GLUT1 expression. NCs treated with 5mM H_2O_2 exhibited an increase in mean intensity (248.0% of control), as well as an increase in sum intensity (234.9% of control), which were both found to be statistically significant.

ECs followed a similar trend to that of NCs in whole cell GLUT1 expression. ECs that were treated with 5mM H_2O_2 displayed an increase in mean intensity (241.5% of control), and an increase in sum intensity (214.5% of control), both significant changes. ACs with H_2O_2 induced injury also showed significant changes in whole cell GLUT1 expression. Mean intensity increased (145.1% of control), while sum intensity increased (127.8% of control) (Figure 7B). These initial results suggest that NCs, ACs and ECs respond to direct ROS injury by increasing GLUT1 expression throughout the cell body, although ACs responded to a lesser extent than NCs and ECs.

In order to confirm this observation, it was also necessary to account for any differential distribution of GLUT1 between the perinuclear region and the rest of the cell cytoplasm. GLUT1 is capable of migrating from intracellular compartments to the plasma membrane [35]. Thus, the fluorescent intensities of only the perinuclear region in 5mM H_2O_2 treated cells were recorded as well, and normalized to the intensities in the perinuclear regions of control cells. NCs and ECs treated with H_2O_2 showed significant increases in GLUT1 perinuclear expression, similar to the increases measured in the entire cell. Mean intensity increased (268.7% of control), while sum intensity increased (277.5% of control) in NCs. ECs increased in mean intensity (229.7% of control), as well as in sum intensity (226.7% of control). Although the mean intensity in ACs significantly increased (134.2% of control), there was a non-significant increase (116.6% of control) in sum intensity (Figure 7C). NCs and ECs followed the same trends of GLUT1 expression

in the perinuclear region as in the entire cell area, while ACs again displayed a much lower increase in expression.

We also sought to observe any relative changes in GLUT1 distribution after ROS injury. The sum intensities of the perinuclear region in H_2O_2 treated cells were normalized to the sum intensities of the entire cell area in H_2O_2 treated cells. These values were then compared to the sum intensities of the perinuclear region in control cells normalized to the entire cell area of control cells. After H_2O_2 treatment, NCs exhibited an increase in perinuclear sum intensity (52.6% to 58.4% of whole cell sum intensity), while ACs exhibited a decrease (43.3% to 39.5% of whole cell sum intensity). ECs displayed a decrease (52.7% to 45.1% of whole cell sum intensity) in perinuclear sum intensity after H_2O_2 treatment (Figure 7D). None of these changes were significant. This indicates that there does not happen to be any significant intracellular migration of GLUT1 in the instance of a direct ROS injury.

After sustaining injury, NCs experience an accelerated energy demand in order to power self repair mechanisms that fix the induced damage [20]. However, as mentioned in Section 2.1, ROS impairs oxidative phosphorylation in the NCs, making it more difficult to create ATP and forcing the NCs to rely on only oxygen-independent glycolysis. Having only glycolysis to work with results in less ATP produced per glucose molecule [6]. This inefficient energy production means that even more glucose is required to obtain a sufficient energy supply. Thus, increased GLUT1 expression is a result of NCs working harder to meet this energy demand by attempting to transport more glucose.

ECs show a proportionally similar increase in GLUT1 expression to that of NCs after direct H_2O_2 treatment likely due to an attempt to address their own energy demands involved in the repair process after lipid peroxidation. It is worth noting that ACs display a less dramatic increase in GLUT1 expression than NCs and ECs in both the entire cell area as well as in only the perinuclear region. Unlike NCs, ACs normally rely on a more glycolytic metabolism [36]. This indicates that ROS interference with the oxidative phosphorylation in an ACs would not cause much hindrance on its energy production. Thus, after injury, the ACs does not have to obtain as much glucose as NCs to produce energy, as the cells' main method of ATP production has not been compromised. This would account for the relatively lower increase in ACs GLUT1 expression.

4.5 Effect of ROS Injury on Cell Viability

Although we observed that ROS injury affected both the cell's morphology and the localization of the GLUT1 transporter, it is unclear how the livelihood of the cell is impacted as a whole. In order to answer this question, we utilized fluorescence microscopy to examine the effects of H_2O_2 on the overall viability of NCs, ECs, and ACs. After the injured cells were incubated with 5 mM H_2O_2 for 15 minutes, cells were treated with Live/Dead fluorescent dyes calcein AM (green) and ethidium homodimer (red) to stain the live and dead cells, respectively. Figure 8A shows images of the cells that were taken by fluorescence microscopy to test their viability.

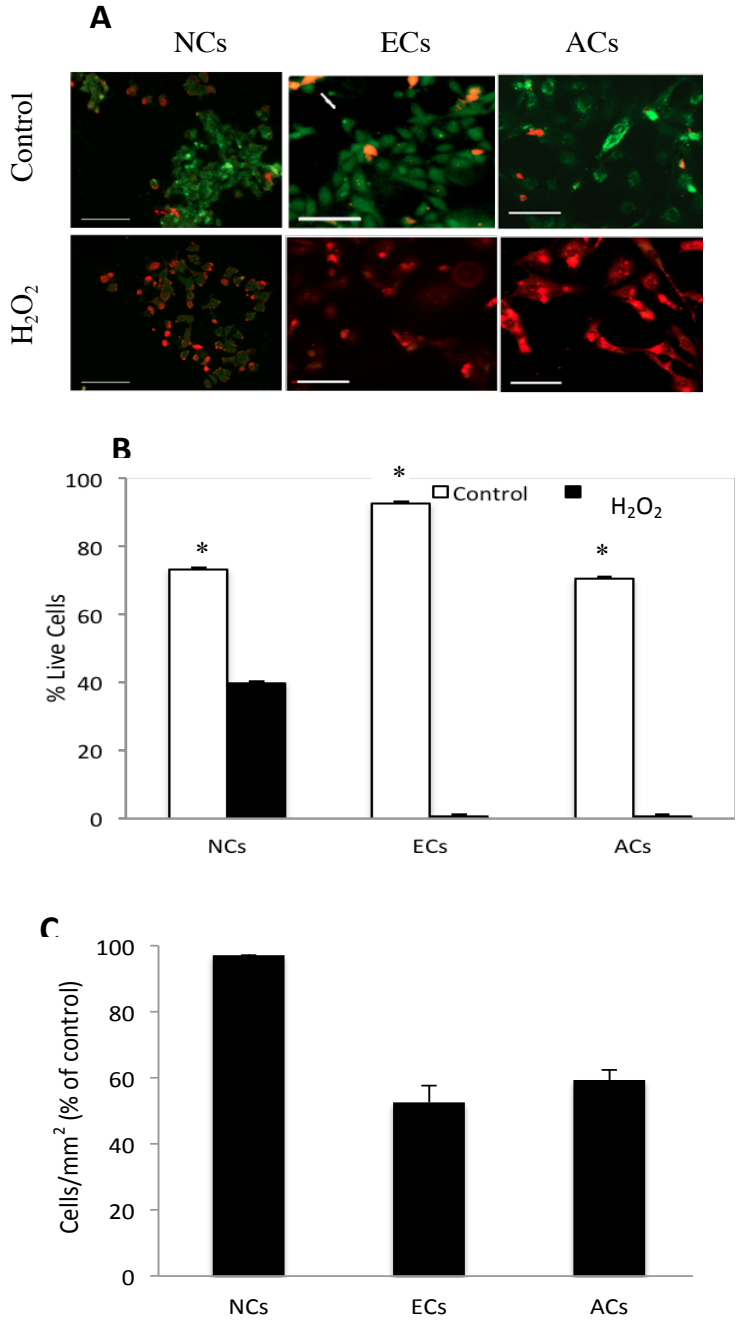

Figure 8. Effect of ROS Injury on Cell Viability.
(A) Experimentation included a control condition and a 5 mM H_2O_2 injury for 15 minutes. Cells are then treated with Live/Dead fluorescent dyes calcein (green) and ethidium homodimer (red) for 15 minutes to stain the live and dead cells, respectively. Images of cells taken by fluorescence microscopy to test viabillity. Scale bars = 100 μm. (B) Quantification of brain cell and BBB cell viability in (A) by comparing the number of live cells between control and injured conditions. (C) The effects of neuronal ROS on brain cells and BBB cell count per mm^2. Data are mean ± SEM. *, Compares H_2O_2 injury to control; $p < 0.05$ by student's *t*-test.

To quantify cell viability after an ROS injury, we compared the number of live cells between the control and injured conditions. Figure 8B shows the percentage of live cells in the control and injured cells. In NCs, we found that 73.1% of cells in the control groups were alive, whereas only 39.7% of control cells were found alive in the 5 mM H_2O_2 injury group. This trend was more notable in the ECs and ACs. The ECs and ACs control groups had 92.4% and 70.3% of cells alive, respectively, while only 0.5% of cells were observed to be alive in both cell types after a 5 mM H_2O_2 injury. This set of experiments demonstrates that the percent live cells is significantly higher in cells that do not undergo H_2O_2 injury.

Another measure of cell viability is the cell density, measured in cells per square millimeter. Figure 7C shows the number of cells per square millimeter in the injured cells, as a percentage of the control cells. The density of NCs was only 102.9% of control in the injured group, whereas the density of ECs and ACs decreased 147.4% of control and 140.6% in the injured group, respectively. The results of Figure 8C agree with the results of 8B in that if more cells die due to treatment and detach from the plate, it would ostensibly follow that there would be less cells left per square millimeter. Figure 8C shows that NCs are much less sensitive than ECs or ACs. Furthermore, these two figures show that ROS injury kills cells and validates the H_2O_2 model.

4.6 Effect of Neuronal ROS Injury on ECs and ACs Morphology

All prior experiments show that direct injury to NCs, ECs and ACs using H_2O_2 has noticeable effects in regard to gross cell morphology, GLUT1 localization, and overall cell viability. However, in a concussion, NCs are the only cell type directly affected, by mechanical stretching of their axons and the resulting OS [6]. ECs and ACs

are located in the same brain environment as the injured NCs; specifically, ECs and ACs compose the BBB, which is surrounded by the brain cells. Therefore, in order to fulfill Aim 2, we examined these same parameters in a model that better represents the brain environment. Our Transwell model (explained in detail in Section 3.2.2) places ECs or ACs in the same environment as injured NCs. We focused on examining whether injury to NCs would propagate to ECs or ACs in a similar manner to directly injuring ECs and ACs in regards to the previously studied parameters.

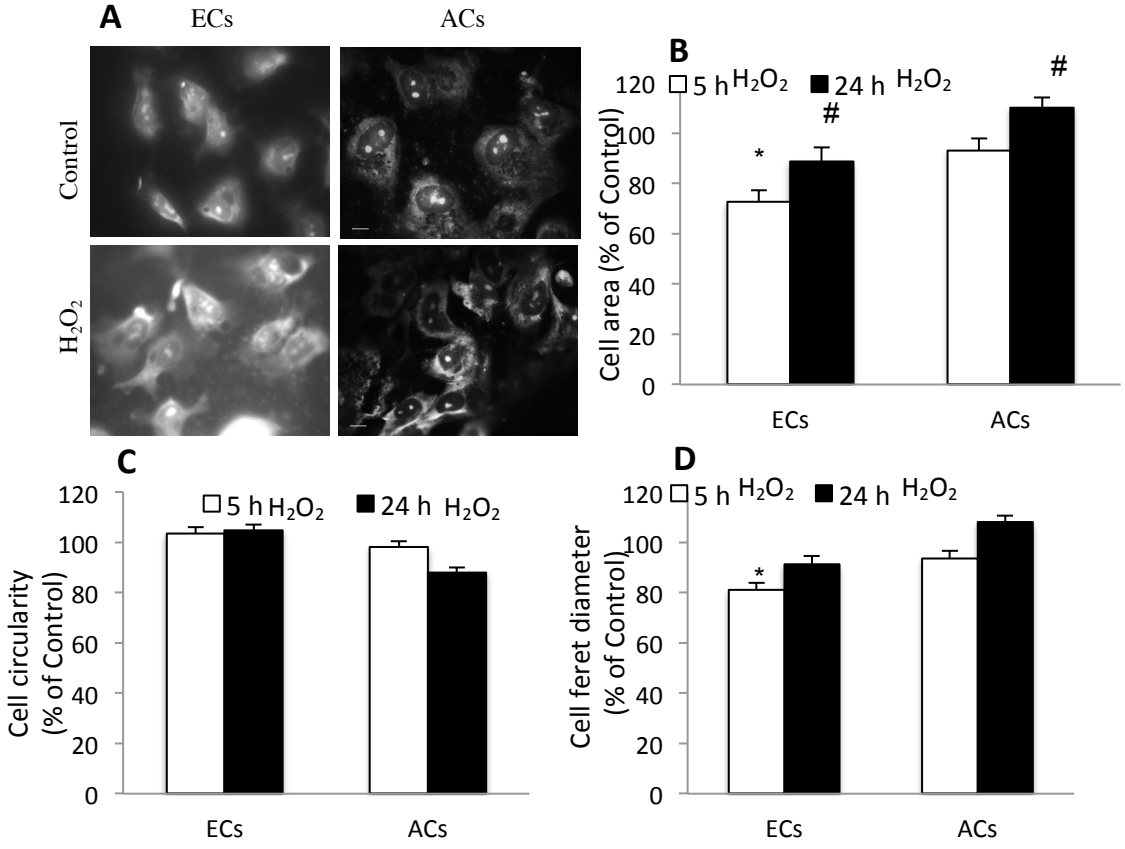

Figure 9. Effect of neuronal ROS injury on EC and AC morphology. (A) Experimentation involved NC incubation with control or 5 mM H_2O_2 solution for 15 minutes. Afterwards, Transwells containing ECs or ACs are placed in the wells with NCs. Images of the ECs and ACs taken via fluorescence microscopy at 60x magnification 5 hours and 24 hours after incubation with treated NCs. Scale bars = 10 μm. (B) Cell area of ECs and ACs 5hrs and 24 hours after incubation with NCs injured with 5mM H_2O_2.

(C) Circularity. (D) Cell Feret diameter. * Compares H_2O_2 injury to control; # compares 5 hour to 24 hour. $p < 0.05$ by student's *t*-test.

To observe morphological changes, we incubated ECs or ACs for 5 or 24 hours with both uninjured and injured NCs. We noted morphological changes in ECs and ACs at 5 hours and 24 hours following the neuronal injury simulated by the 5mM H_2O_2 exposure (Figure 9). ECs decreased in area to 72.6% of control in the 5 hour group, and to 88.7% of control in area in the 24 hour group. ACs in the 5 hour group experienced a decrease in area to 92.9% of control, while those incubated for 24 hours increased to 110.1% of control. There were no significant effects on the circularity of the ECs at either time point, while the ACs only decreased to 87.9% of control in circularity in the 24 hour group (Figure 9C). Figure 9D shows that the Feret diameter trends vary similarly to cell area with respect to both ECs and ACs. For ECs, Feret diameter was 81.1% of control in the 5 hour group, and 91.3% of control in the 24 hour group. For ACs, Feret diameter was 93.6% of control in the 5 hour group and 92.1% of control in the 24 hour group. Overall, the ECs decreased in size over time, but did not significantly change in shape as a result of the neuronal injury.

Based on the aggregate data, the ECs at 24 hours were less affected compared to 5 hours. The mechanism behind this is unclear, but it may be due to the rate of propagation of ECs and stabilization after the shock of the injury to begin of the recovery process. This also may hold true to a greater extent with regards to the ACs. In the 24 hour group, the ACs seemed to have reverted from shrinkage, initially due to the release of glycogen [24], to display an increase in cell area and Feret diameter. It is plausible that this could be due to the role of the ACs in the brain; specifically, it is suggested that damage causes

a reaction for the cells to suspend in initial growth phase to produce neural growth factor in order to help damaged NCs recuperate [37]. The resulting data suggests ACs recovery and outgrowth may be a byproduct of this phenomenon.

4.7 Effect of Neuronal ROS Injury on EC and AC GLUT1 Localization

Having observed the effects of direct ROS injury upon cells in previous GLUT1 localization experiments, we utilized fluorescence microscopy to investigate whether ECs or ACs incubated with NCs that have been treated for 15 minutes with 5 mM H_2O_2 demonstrated changes in GLUT1 expression. The results of the morphology analysis showed the ECs and ACs had greater changes in the 5 hour group and the 24 hour group, respectively. Therefore, for the following localization experiments, ECs were incubated for 5 hours, while ACs were incubated for 24 hours. ECs and ACs were immunostained with a GLUT1 mouse anti-human antibody, followed by a FITC-conjugated goat-anti-mouse antibody (Figure 10A). As in Section 4.4, the mean (expression per unit area) and sum (total expression) intensities of the GLUT1 fluorescence were then measured and normalized relative to the control condition.

In entire cell area fluorescent measurements, ECs did not display significant changes for GLUT1 expression; mean intensity decreased (95.5% of control) while the sum intensity increased (103.9% of control). ACs showed a decrease in mean intensity (84.4% of control), along with a decrease (77.7% of control) in sum intensity. Both these changes were significant, suggesting a decrease in GLUT1 expression following exposure to NCs injured with H_2O_2 (Figure 10B). These trends were consistent when accounting for differential distribution of GLUT1 by measuring fluorescence in only the perinuclear region. In this region, ECs indicated a decrease in mean intensity (83.9% of

control), and an increase in sum intensity (103.1% of control), which were both non-significant changes. Thus, there was no significant alteration in GLUT1 expression in any part of the ECs. ACs displayed significant decreases in perinuclear mean intensity (83.1% of control) and the perinuclear sum intensity decreased (84.7% of control) (Figure 10C), confirming lowered GLUT1 expression all throughout the cell.

When comparing the perinuclear sum intensities of control and injured cells, normalized to the whole cell sum intensities of their respective conditions, there were non-significant changes. The perinuclear sum intensity of ECs decreased (50.6% to 50.5% of whole cell sum intensity) as a result of H_2O_2 injury, while the perinuclear sum intensity of ACs rose (42.8% to 46.6% of whole cell sum intensity). This signifies that after H_2O_2 injury, GLUT1 did not redistribute to other parts of the cell in both ECs and ACs, even though the ACs as a whole expressed less GLUT1. In previous localization experiments, ECs that directly suffered a 5 mM H_2O_2 injury expressed a significantly higher amount of GLUT1, while ACs expressed a relatively less steep expression increase in response to such an injury.

In these experiments, ECs exposed to NCs that have suffered a 5 mM H_2O_2 injury did not display any changes in GLUT1 expression, while ACs exposed to damaged NCs exhibited significant decreases in expression. This disparity in expression behavior between the two sets of experiments can be attributed to the presence of the damaged NCs. It was previously mentioned that when NCs are damaged, they experience a spike in energy metabolism in order to fuel their repair mechanisms and restore cell health [20]. NCs, compromised by ROS injury, likely send signals of their injury to other nearby cells (either ECs or ACs) so that these other cells may aid in meeting this energy demand. ECs

comprise the brain vasculature, and are mainly involved in transporting molecules [23]. They may not be capable of providing energy to the NCs hypermetabolism. This results in the inability by the ECs to respond to NCs injury signals and thus the lack of change in GLUT1 expression. ACs are known to store glucose and transfer this energy to NCs that cannot meet energy requirements with their own supply [26]. Based on this knowledge, GLUT1 expression should hypothetically increase in ACs to help meet NC metabolic demand. However, the decrease in GLUT1 expression found in ACs disagrees with this idea. Facing this dilemma, we then returned to the data and compared the sum intensities of ECs and ACs after incubation with injured NCs. In control conditions, AC sum intensity was significantly higher that of ECs, signifying overall higher GLUT1 expression in ACs. This finding suggests that ACs possessed basal expression levels of GLUT1 that may be high enough to support NC injury-related hypermetabolism without having to increase GLUT1 expression any further. The reason for the AC decrease in expression may then be attributed to cell shrinkage after exposure to injured NCs. Figure 9B displays a cell area decrease in ACs after 5 hours of incubation with injured NCs, then a recovery of cell area after 24 hours of incubation with injured NCs. Somewhere between the start of incubation and the 24 hour time point, the AC shrank, which may be related to cell apoptosis and loss of cell biomolecules (including GLUT1).

Figure 10. Effect of neuronal ROS injury on EC and AC GLUT1 localization. (A) Experimentation included a control and 5 mM H_2O_2 injury to the NCs in the Transwells for 15 minutes. Afterwards, GLUT1 was immunostained in ECs and ACs using a primary and FITC-secondary antibody. Images of samples were taken by fluorescence microscopy on the FITC and DAPI (nucleus) channels at 60x magnification. FITC staining achieves the green color, representing GLUT1 expression and the blue color, represents cell nuclei. Scale bars = 10 μm. (B) Quantification of mean and sum intensity in cells incubated with injured NCs expressed as a percentage of cells exposed to control NCs. (C) Quantification of mean and sum intensity corresponding to the perinuclear area of cells incubated injured NCs expressed as a percentage of intensities in cells exposed to control NCs. (D) Quantification of sum intensity in the perinuclear region expressed as a percentage of the whole cell sum intensity. Data are mean ± SEM. *, Compares 5mM H_2O_2 injury to control . $^{\#}$, Compares ACs to ECs; $p < 0.05$ by student's *t*-test.

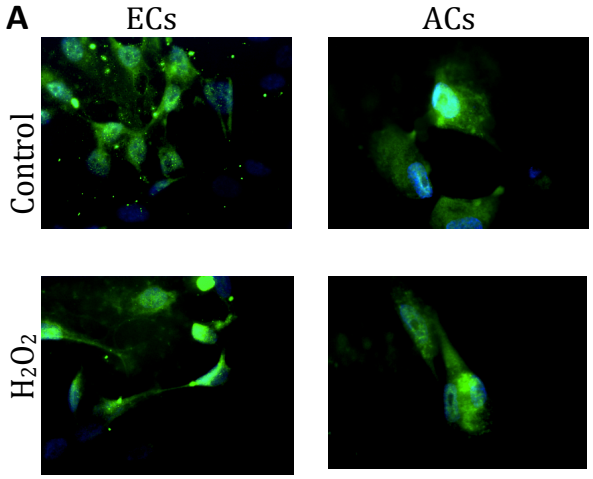

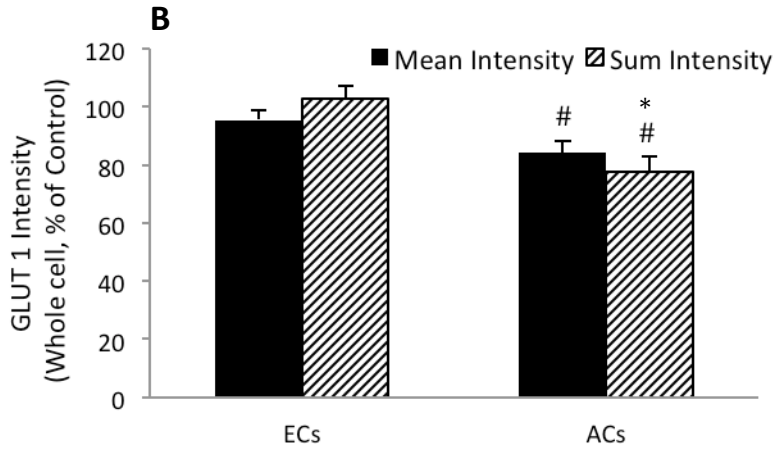

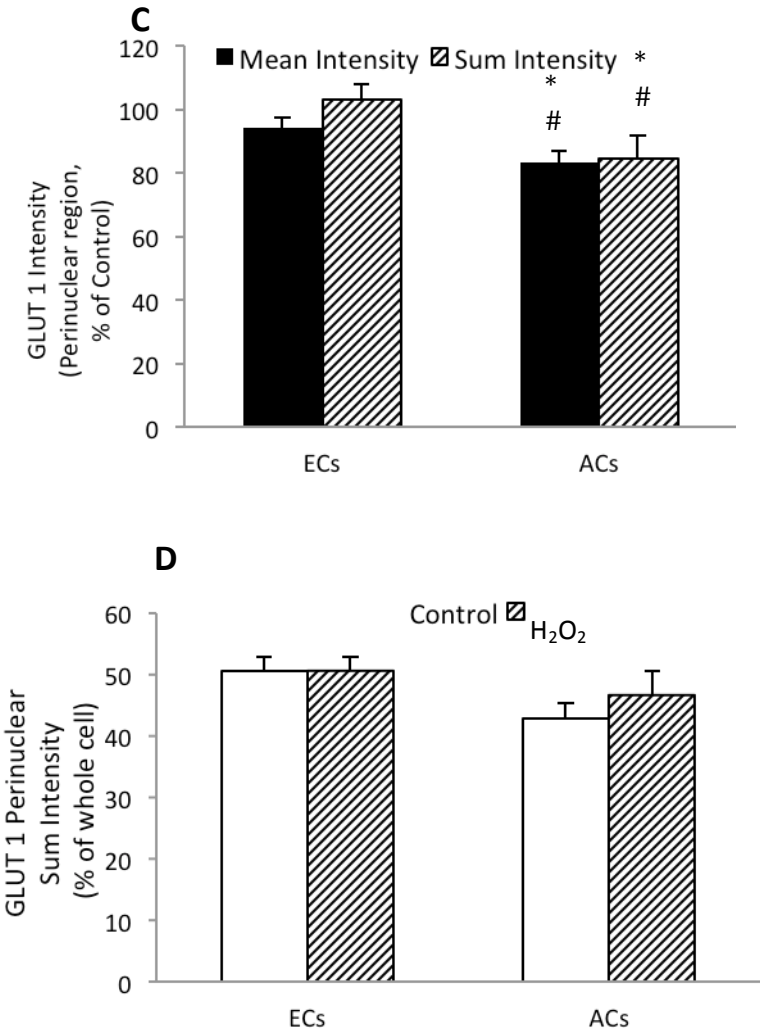

4.8 Effect of Neuronal ROS Injury on EC and AC Viability

Since we observed that a neuronal ROS injury affects both cell morphology and the localization of the GLUT1 transporter, and past experiments demonstrated that an ROS injury affects the viability of cells individually, we continued our experimentation by utilizing microscopy to analyze the effect of H_2O_2 on cell viability in the Transwell co-culture model. In addition to examining the responses of different cell types, we also evaluated the cell viability at two different time points, 5 hours and 24 hours, in both ECs and ACs, after H_2O_2 injury.

To quantify the cell viability of NCs, ECs, and ACs after the NCs are injured in this Transwell model, we compared the number of live cells between the control cells and 5 and 24 hours after the injury, as shown in Figure 11A. We found 86.8% of NCs were alive in the control experiments, whereas only 68.5% of ECs were alive and 65.6% of ACs were alive. Five hours after the injury, we found 17.4% NCs, 23.5% ECs, and 40.6% ACs were alive. This suggests that the damage from a neuronal ROS injury propagates to ECs and ACs. In accordance with the data, we would expect NCs to have the lowest cell viability, since NCs are the cell type that directly receives the H_2O_2 injury. We see a similar overall trend 24 hours after injury, where we found only 14.3% of NCs, 37.7% of ECs, and 26.7% of ACs.

A potential explanation for why ECs have a higher viability in the 24 hour group than the 5 hour group could be attributed to the fact that cells that survive the injury may continue to divide. This trend is not observed for NCs and ACs, both of which have cells alive in the 24 hour group, as compared to the 5 hour group.

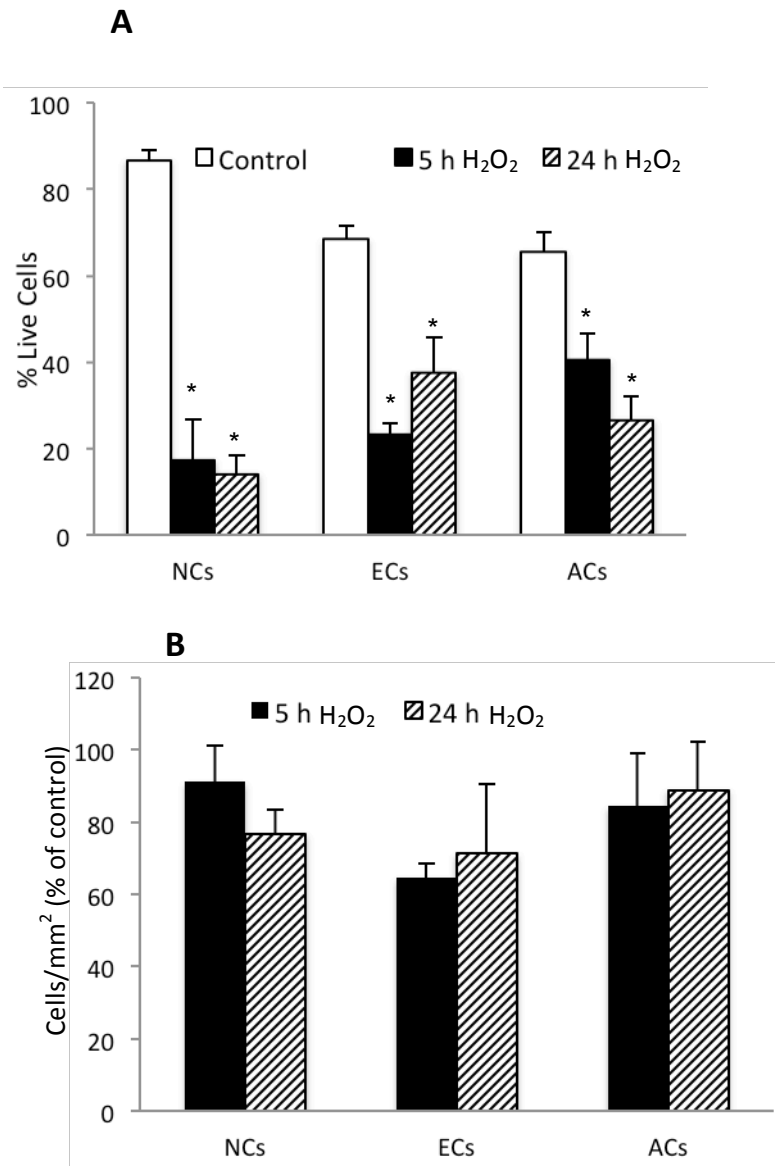

Figure 11. Effect of neuronal ROS injury on EC and AC viability. (A) The effects of neuronal ROS on the viability of NCs, ECs, and ACs 5 hours or 24 hours after exposure of NCs to 5 mM H_2O_2. Cells were incubated for 15 minutes with trypan blue dye at 37°C and viability was then tested and analyzed by manually counting cells on a hemocytometer at time points 5 hours and 24 hours after the 5 mM H_2O_2 injury. (B) The effects of neuronal ROS on EC and AC cell count per unit area 5 hours and 24 hours after the H_2O_2 injury, as a percentage of the cells exposed to control NCs. Data are mean ± SEM. *, Compares H_2O_2 injury to control; $p < 0.05$ by student's *t*-test.

Another measure of cell viability in this experiment is cell density, measured in the amount of cells per square millimeter. Figure 11B shows the number of cells per square millimeter in the NCs, ECs, and ACs, when incubated with the injured NCs, as a percentage of the number of cells per square millimeter in control cells. Five hours after the H_2O_2 injury to NCs, the density of NCs decreased 8.8%, where the density of ECs decreased 35.3%, and the density of ACs decreased 15.5%. 24 hours after the injury to the NCs, NCs had 76.7% as a percent of control, where ECs had 71.3% and ACs had 88.9%. The results of Figure 11B agree with the results of 11A: the results displayed in Figure 11B suggest ECs and ACs are able to divide after exposure to neuronal ROS, increasing the number of cells per square millimeter. Figure 11A shows that NCs are significantly more sensitive to a H_2O_2 injury than ECs or ACs that are incubated with injured NCs, since there are far fewer live NCs after the neuronal injury. We observed that injured NCs in a co-culture model are more sensitive than NCs injured in monoculture (in section 4.5), which suggests that the cellular interactions between NCs and either ECs or ACs in co-culture cause NCs to experience a greater impact from the injury when compared to the individually injured NCs.

CHAPTER 5: CONCLUSION AND FUTURE DIRECTIONS

As a consequence of the altered ion channels caused by axonal stretching during concussion, ROS is overproduced. Increased ROS levels hinder cellular ability to perform glycolysis, the body's primary function for converting glucose to ATP by damaging major cellular components, ultimately disrupting the recovery time from a concussion while hindering physiological performance [6,9]. Many concussion

symptoms, such as headaches, memory loss, changing sleep patterns, and emotional instability, stem from the overproduction of ROS in NCs affecting the cell's ability to perform basic functions. Our research focused on the effects of ROS in NCs after the incidence of a concussion. We hypothesize that ROS creates independent alterations in NCs, ECs, and ACs, and also that effects of ROS produced in NC cells propagate to ECs and ACs. Specifically, we looked into the effects of ROS on cellular morphology, neuronal viability, and glucose transporter expression and localization.

Our investigation addresses the prevalence of ROS in causing neuronal deterioration as well as causing subsequent changes in ACs and ECs. Using H_2O_2 to mimic the production of ROS, initial experimentation confirmed the basic concept behind our model, finding that concentrations of H_2O_2 consistently induced significant ROS levels in NCs, ECs and ACs. With this model validation, we were able to begin research into the pathophysiology of concussion.

We first focused on assessing the impact of ROS on the morphology of NCs, ECs, and ACs. For the purposes of our research, this included parameters to quantify the potential alterations in size and shape, as well as the status of cell confluency. Cells were exposed to different concentrations of H_2O_2 for 15 minutes and changes in morphology were examined by microscopy. This exposure to H_2O_2 aims to mimic the ROS injury sustained during a concussion and allows us to test our hypothesis in a cell culture model. Injured cells were shown to decrease in surface area, signifying a shriveling effect when cells are exposed to ROS. In addition, gap between cells also increased as well, further depicting gross level structural changes in injured cells.

After assessing the effects of ROS production within NCs, experimentation shifted to a Transwell model, simulating the BBB and the interactions between cells during the injury. We analyzed the morphological effects of NC ROS injury on ECs and ACs. This quantifies the propagation of injury from NCs to ECs and ACs. Using H_2O_2 to injure NCs, our results showed that ECs tend to shrink over the 24 hours following injury, but do not change in shape. However for ACs, their initial reduction in size is not long lasting, fully recovering by the 24 hour mark.

Knowing that the ROS injury can influence morphological parameters of brain cells, the next step was to evaluate the changes to GLUT1 expression. This is important because glucose metabolism is paramount during periods of high OS, such as during a concussion. In order to assess the effect of ROS production on GLUT1 expression in NCs, ECs, and ACs, we quantified the ratio of GLUT1 to GAPDH. There was a dose dependent increase in GLUT1 expression seen in NCs and ECs, as well as an inverse dose dependent increase in ACs. However, extremely large levels of variability between trials rendered these results non-significant.

Given this, our next step was to determine the protein expression within cells in response to ROS overproduction. Both NCs and ECs displayed a significant increase in both mean and relative intensity. This illustrates the idea that more GLUT1 transporters are produced in cells undergoing stress related to ROS. However, ACs did not follow suit, with very minimal and non-significant changes in mean and sum intensity, consistent with previous studies claiming GLUT1 is prioritized less in ACs. In order to quantify the accuracy of our findings, we also observed the distribution of GLUT1 in the perinuclear region because it is known that this transporter can be mobilized from the

intracellular region to plasma membrane regions [38]. This analysis showed an increase in GLUT1 in response to the ROS generated during injury. These findings are also consistent with the notion that concussive injury creates a higher glucose demand in order to repair the damaged NCs. In addition, AC trials displayed minimal changes in mean and sum intensity, just as for the whole cell.

After observing the presence of GLUT1 in ACs and ECs, the effect on GLUT1 levels and distribution were examined after incubating each of these cell types in injured NCs. This assesses the pathophysiological response to concussion, quantifying the amount of glucose transporter available during the brain's energy deficit. In our Transwell model, our results reflect the impact of NC ROS in inducing subsequent cell injury. After injuring NCs, the ACs GLUT1 intensity significantly decreased in sum and mean intensity; however, EC intensity showed a much more modest sum and mean intensity decrease. This relates to the differences between ECs and ACs in the post-injury environment. ACs are known to store glucose and transfer this to the injured NC cell to help make up its own [26]. Contrarily, ECs may not be involved in providing their own glucose to NCs during the hypermetabolic state. As a result, the distribution of GLUT1 that we observed in the study for these respective cell types follows the existing literature. In terms of perinuclear GLUT1 distribution, this followed the same trend, with the mean and sum intensity for ECs and ACs decreasing. This once again relates to the ability of ECs and ACs to reallocate glucose to the NC energy deficit. Although these correlations are promising, GLUT1 expression for live and dead cells was not differentiated in these trials, which is something that can be examined in future works.

After understanding the impact of ROS injury on GLUT1 localization and cellular morphology, the final step was to identify its influence on cellular viability. In order to determine the effectiveness of our injury model, NCs, ECs, and ACs were injured with H_2O_2. From this, we discovered that ROS injury decreases cell viability in all three cell types. With our experimental conditions in single cell culture, ECs and ACs showed very little viability, while neurons showed more resilience to the ROS injury. After arriving at this conclusion, we shifted analysis to determining the effect of NC ROS injury propagating to ECs and ACs. Using 5 hours and 24 hours as the two points of study, we are able to assess cell viability after the ROS injury. For both post-injury time points, we found fewer live cells compared to the control across all three cell types. In these trials, NCs were the most sensitive to ROS, exhibiting the greatest effect on cell viability for both time points; an expected outcome as they were the only cell type to be directly injured with ROS. While ECs and ACs both experienced a decrease in viability after being exposed to the injured NCs, ACs were less sensitive and exhibited a higher percentage of surviving cells. These results illustrate that ROS injury can spread via some biochemical mechanism from NCs to the ACs and ECs. The nature of this possible intercellular communication is not specifically known, but it may be a particular type of ROS or other molecule that is released to signal the other cells. Not only the effects of NC injury propagate to other cells, but also NCs were the most sensitive to ROS injury in the Transwell model, rather than ECs and ACs exposed to injured NCs. This suggests that the interaction between NCs and other cells in the BBB also may play a role in causing ROS injury for NCs.

In summary, using an H_2O_2 injury model, our research has demonstrated that ROS has detrimental and significant effects on the overall health of NCs, ECs, and ACs. Our results also suggest that the effects of ROS originating in NCs can later propagate to ECs and ACs in culture. This propagation shows widespread changes in ECs and ACs that are very similar to that of ROS imparted directly upon these cells.

Future research avenues would explore the effects of injuring NCs in a manner more directly similar to a concussion injury; that is, via a mechanical stretching of the axon. The Cell Injury Controller II, created by researchers at Virginia Commonwealth University, is designed to create a diffuse axonal injury (DAI) that mimics the physiological symptoms of concussion in a cellular model [39]. The Controller imparts controlled blasts of air upon NCs plated on Flexwell cell culture plates, which include a silastic bottom in which the axons of the NCs can be stretched in a consistent manner [39]. This mechanism would induce ROS in the same manner a concussion would, and would address GLUT1 expression and localization, as well as gross cell morphology and cell viability in a manner more relevant to the actual pathology of a concussion.

More advanced *in vivo* research could take this premise further, and directly concuss a mouse animal model. Arguably the most viable model for a mild traumatic brain injury would be via the weight drop method on a mouse, in which the skull of the animal is exposed, and it is subjected to a free falling, guided weight that is designed to elicit a brain injury [40]. After concussion via the weight drop, the brain of the animal would be harvested, and cultures of each of the cell types would be prepared. These cultures could then be manipulated and examined in regards to each of the parameters discussed in the present study.

Further examination of the three cell types that were studied would be possible by examining expression of both the GLUT3 transport protein and the hexokinase enzyme. Although GLUT1 is the primary transporter of glucose in ECs and ACs, the GLUT3 transporter is responsible for the majority of glucose transport of NCs [24]. During times of high stress, such as under high levels of ROS, the GLUT3 transporter is responsible for rapidly bringing glucose into the cell, in order to restore homeostasis [24]. It is worth looking into whether GLUT3 expression in the three cell types is affected by ROS in a similar manner to GLUT1. Furthermore, expression of the hexokinase enzyme may also be affected when cells are affected by ROS, as cells under stress may produce more hexokinase in order to more efficiently metabolize glucose via cellular respiration. It may be worth examining differential expression of hexokinase as well in the three cell types in the same multi-culture model. Another possible direction would be to utilize a glucose assay in order to quantify the levels of glucose in the three cell types. This could garner further insight on the metabolic activity of the cells in relation to the expression of the glucose transport proteins GLUT1 and GLUT3.

Ultimately, a comprehension of how BBB cell types are affected during ROS injury has sizable implications towards our understanding of concussions. Elucidating how injury to NCs results in drastic physiological changes in ECs and ACs demonstrates the oft-underestimated dangers of concussion on a cellular level. The fact that injury to NCs can indirectly and severely affect the functioning of BBB cells that support them is valuable grounds for further research. It emphasizes the idea that concussions cause a rapid change in the entire brain environment, causing a cascade that travels far beyond

the initial point of injury, propagating through the entirety of the cerebral cortex and resulting in widespread damage.

CHAPTER 6: REFERENCES

[1] L. Gessel, S. Fields, C. Collins, R.W. Dick, R.D. Comstock, Concussions among United States high school and collegiate athletes, J Athl Train. 42 (2007) 495-503.
[2] M.J. Ellis, J. Leiter, T. Hall, P.J. McDonald, S. Sawyer, N. Silver, M. Bunge, M. Essig, Neuroimaging findings in pediatric sports-related concussion, J Pediatr Neurosci. 16 (2015) 241-247.
[3] L. Smith-Seemiller, N.R. Fow, R. Kant, M.D. Frazen, Presence of post-concussion syndrome symptoms in patients with chronic pain vs mild traumatic brain injury, Brain Inj. 17 (2003) 199-206.
[4] Signs and Sypmtoms, Injury Prevention & Control: Traumatic Brain Injury & Concussion. (2016). https://www.cdc.gov/traumaticbraininjury/symptoms.html (accessed March 1, 2016).
[5] A.K. Shetty, V. Mishra, M. Kodali, B. Hattiangady, Blood brain barrier dysfuction and delayed neurological deficits in mild traumatic brain injury induced by blast shock waves, Front Cell Neurosci. 8 (2014) 105-114.
[6] S. Signoretti, G. Lazzarino, B. Tavazzi, R. Vagnozzi, The Pathophysiology of Concussion, PM&R. 3 (2011) S359-S368.
[7] A.L. Petraglia, E.A. Winkler, J.E. Bailes, Stuck at the bench: Potential natural neuroprotective compounds for concussion, Surg Neurol Int. 2 (2011) 146.
[8] J.A. Joseph, B. Shukitt-Hale, G. Casadesus, D. Fisher, Oxidative stress and inflammation in brain aging: nutritional consideration, Neurochem Res. 30 (2005) 927-935.
[9] E. Birben, U.M. Sahiner, C. Sackesen, S. Erzurum, O Kalayci, Oxidative Stress and Antioxidant Defense, World Allergy Organ J, 5 (2012) 9-19.
[10] G. Barkhoudarian, D.A. Hovda, C.C. Giza, The molecular pathophysiology of concussive brain injury, Clin Sports Med. 30 (2011) 33-48.
[11] Y. Itoh, T. Abe, R. Takaoka, N. Tanahashi, Fluorometric determination of glucose utilization in neurons in vitro and in vivo, J Cereb Blood Flow Metab. 24 (2004) 993-1003.
[12] S. Muro, Strategies for delivery of therapeutics into the central nervous system for treatment of lysosomal storage disorders, Drug Deliv Transl Res. 2 (2012) 169-186.
[13] R. Smith, M. Murphy, Animal and human studies with the mitochondria-targeted antioxidant MitoQ, Ann NY Acad Sci. 1201 (2010) 96-103
[14] H.C. Helms, N.J. Abbott, M. Burek, R. Cecchelli, In vitro models of blood-brain barrier: An overview of commonly used brain endothelial cell culture models and guidelines for their use, J Cereb Blood Flow Metab. (2016) 1-29.
[15] I. Wilhelm, C. Fazakas, I.A. Krizbai, *In vitro* models of the blood-brain barrier, Acta Neurobiol. 71 (2011) 113-128.

[16] A.M. Enciu, M. Gherghiceanu, B.O. Popescu, Triggers and effectors of oxidative stress at blood-breain barrier level: revelance for brain aging and neurodegeneration, Oxid Med Cell Longev. 2013 (2013) 1-12.
[17] M. Fransen, M. Nordgren, B. Wang, O. Apanasets, Role of peroxisomes in ROS/RNS-metabolism: Implications for human disease, Biochim Biophys. 1822 (2012) 1363-1373.
[18] M. Giorgio, M. Trinei, E. Migliaccio, P.G. Pelicci, Hydrogen peroxide: a metabolic or a common mediator of aging signals?, Nat Rev Mol Cell Biol. 8 (2007) 722-728.
[19] C.P. Chih, E.L. Roberts Jr, Energy substrates for neurons during neural activity: a critical review of the astrocyte-neuron lactat shuttle hypothesis, J Cereb Blood Flow Metab. 23 (2003) 1263-1281.
[20] C.C. Giza, D.A. Hovda, The Neurometabolic Cascade of Concussion, J Athl Train. 36 (2001) 228-235.
[21] T. Peng, M. Jou, Oxidative stress caused by mitochondrial calcium overload, Ann NY Acad Sci. 1201 (2010) 183-188.
[22] P. Ballabh, A Braun, M. Nedergaard, The blood-brain barrier: an overview: structure, regulation, and clinical implications, Neurobiol Dis. 16 (2004) 1-13.
[23] R. Gabathuler, Approaches to transport therapeutic durgs across the blood-brain barrier to treat brain disease, Neurobiol Dis. 37 (2010) 48-57.
[24] S.J. Vannucci, F. Maher, I.A. Simpson, Glucose transporter proteins in brain: delivery of glucose to nerons and glia, Glia. 21 (1997) 2-21.
[25] M.V. Sofroniew, H.V. Vinters, Astrocytes: biology and pathology, Acta Neuropathol, 119 (2010) 7-35.
[26] A.M. Brown, B.R. Ransom, Astrocyte glycogen and brain energy metabolism, Glia. 55 (2007) 1263-1271.
[27] J. Hsu, J. Rappaport, S. Muro, Specific Binding, Uptake, and Transport of ICAM-1-Targeted Nanocarriers Across Endothelial and Subendothelial Cell Components of the Blood-Brain Barrier, Pharm Res. 31 (2014) 1855-1866.
[28] A. Gimenes-Cassina, F. Lim, J. Diaz-Nido, Differentiation of a human neuroblastoma into neuron-like cells increases their susceptibility to transduction by herpesviral vectors, J Neuro Res. 84 (2006) 755-767.
[29] K. Hatherell, P.O. Couraud, I.A. Romero, B. Weksler, G.J. Pilkington, Development of a three-dimensional, all-human in vitro model of the blood-brain barrier using mono-, co-, and tri- cultivation Transwell models, J Neurosci Methods. 199 (2011) 223-229.
[30] M. Zhang, G. Xu, W. Liu, Y. Ni, W. Zhou, Role of Fractalkine/CX3CR1 Interaction in Light-Induced Photoreceptor Degeneration through Regulating Retinal Microglial Activation and Migration, PLoS One. 7(2012) 1-12.
[31] CellROX® Green Reagent, for oxidative stress detection. https://www.thermofisher.com/order/catalog/product/c10444 (accessed February 8, 2014).

[32] D.M. Chudakov, V.V. Belousov, A.G. Zaraisky, A.G. Novoselov, Kindling fluorescent proteins for precise *in vivo* photolabeling, Nat Biotech. 21 (2003) 191-194.
[33] C.H. Coyle, Mechanisms of H_2O_2-Induced oxidative stress in endothelial cells, RadicBio Med. 40 (2006) 2206-2213.
[34] K. Satoh, S. Godo, H. Saito, B. Enkhjargal, H. Shimokawa, Dual Roles of Vascular-derived Reactive Oxygen Species—With a Special Reference to Hydrogen Peroxide and Cyclophilin A, J Mol Cell Cardio. 73 (2014) 50-56.
[35] Y. Maeda, H. Terasawa, Y. Tanaka, C. Mitsuura, K. Nakashima, Separate cellular localizations of HTLV-1 Env and GLUT1 are required for HTLV-1 Env-mediated fusion and infection, J Virology. 89 (2015) 502-511.
[36] D.A. Turner, D.C. Adamson, Neuronal-Astrocyte Metabolic Interactions: Understanding the Transition into Abdormal Astrocytoma Metabolism, J Neuropathol Exp Neurol. 70 (2011) 167-176.
[37] A.B. Cragnolini, M. Volosin, Y. Huang, W.J. Friedman, Nerve growth factor induces cell cycle arrest of astrocytes, Devl Neurobiol. 72 (2012) 766-776.
[38] N. Kozlovsky, A. Rudich, R. Potashnik, Y. Ebina, T. Murakami, B. Bashan, Transcriptional Activation of the *Glut1* Gene in Response to Oxidative Stress in L6 Myotubes, J Biol Chem. 272 (1997) 33367-33372.
[39] E.F. Ellis, J.S. McKinney, K.A. Willoughby, S. Liang, & J.T. Povlishock, A new model for rapid stretch-induced injury of cells in culture: characterization of the model using astrocytes, J Neurotrauma. 12 (1995) 325-339.
[40] Y. Xiong, A. Mahmood, M. Chopp, Animal models of traumatic brain injury, Nat Rev Neurosci. 14 (2013) 128-142.

APPENDIX

A. ROS Detailed Monocellular Model Protocol

1) Wash wells with filtered RPMI (300 µL/well)
2) Add 300 µL warm 5mM H2O2 (in RPMI) to wells
3) Incubate for 15 minutes at 37 C
4) Drain H2O2, wash cells using warm filtered RPMI (300 µL/well)
5) Add in dye mix – 300 µL into well
    a) Dye:
        i) Dilution- 16 µL of 2.5 mM stock ROS dye + 7984 µL PBS
        ii) Will result in 8mL of 5 µM ROS dye
6) Incubate 15 min at 37 degrees Celsius
7) Drain dye and wash with PBS(-) (300 µL)
8) Fix with cold 2% PFA (300 µL in transwel)
9) Incubate 15 minutes at room temperature.
10) Drain PFA, then wash with PBS(-) (300 µL)
11) Mount
    a) Place 4 µL Mowiol on slide
    b) Place coverslip(cell side facing up) onto Mowiol

Mounting regularly on slide:

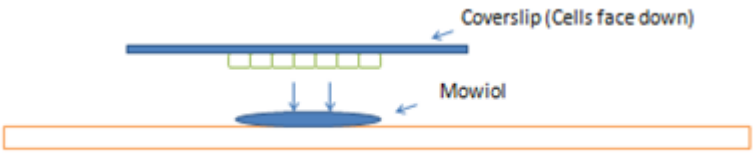

B. Morphology Detailed Monocellular Model Protocol

1) After removing cells from incubator:
2) Wash cells 1x w/ warm RPMI (1 mL)
3) Add 300 µL phenol red free RPMI to control wells. Add 300 µL 5mM H2O2 to injured wells
   a) 1st dilution (100mM H2O2) : 9898 µL PBS + 102 µL stock H2O2 (9.82 M)
   b) 2nd dilution: 9500 µL PBS + 500 µL of (100mM H2O2) = 10 mL of 5mM H2O2
4) Incubate for 15 min. @ 37 Celsius in non-sterile incubator
5) Wash cells 1x w/ warm RPMI (1 mL).
6) Fix cells w/ 300 µL PFA for 15 min. @ RT
7) Wash cells 1x w/ PBS (1 mL)
8) Mount cells using 4 µL Mowiol directly placed on cover slip

Mounting regularly on slide:

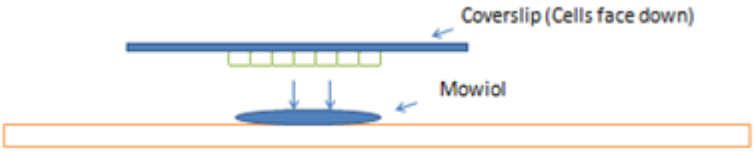

Protocol for analyzing cell morphology in ImageJ:

1) Open ImageJ, File - Open image to analyze
2) Go to Analyze - Set Measurements, check: Area, Feret Diameter, Shape descriptors, Add to overlay. Everything else can be left unchecked.
3) Go to Analyze - Set Scale, for 60x pictures: Distance in pixels- 1, Known distance 0.1075. Set Unit of length to microns, and check Global so you don't have to repeat this for every picture
4) To give the image a scale bar click Analyze – Tools - Scale bar
5) Select Freehand Selections (Bean shaped Icon on the toolbar)
6) Manually trace the shape of a cell
7) Click Analyze - Measure (Ctrl+M), a Results window will pop up, you will want to keep track of this. Specifically, the main parameters of importance are Area, Circ. (circularity), and Feret. The other ones that show up in the table can be left out when organizing data.
8) Repeat until you have all of your desired measurements for the picture. Save the labelled image as a new picture so you can keep an original unedited copy of the image.
9) Once you have finished measuring all your images, you can simply export the results by saving it as a spreadsheet.
10) Keep each condition in a separate results tab, making sure to close the previous tab when going on to the next trial.

Measuring Cell Gap: (do this separately from the cell tracing as not to clutter up your Results tab)

1) Select the Straight line icon on the toolbar
2) Find what you think is the largest gap in between any two adjacent/connected/nearby cells (use your judgment)

3) Click Analyze - Measure, the gap will be shown as ‘Length’ in the Results tab
4) Repeat until you have your desired measurements, save, and export your results.

Quantifying Results

Take the four parameters and compile them into one spreadsheet, calculate mean, standard deviation and standard error for all of them. Then, use a two-tailed t-test to see whether there are significant differences between the control and the experimental groups, as well as between the experimental groups.

C. Morphology Detailed Transwell Model Protocol

1) Remove cells from incubator, drain media. Wash with 500 uL RPMI at room temp, 2x.
2) Treat cells with 300 uL of 0mM (control), 0.5mM, and 5mM concentrations of H_2O_2 diluted in RPMI, incubate at 37*C for 15 minutes (put back into incubator)
3) Drain media, wash cells again with 500 uL RPMI at room temp, 3x.
4) Fix cells with cold 2% PFA in PBS, incubate for 15 minutes at room temp.
5) Drain wells, wash cells with 500 uL PBS at room temp, 3x.
6) Remove coverslips from wells and mount onto slides with moiwol
   a) Use a razor blade to cut out the cell insert on the Transwell
   b) Place 4 µL Mowiol on slide
   c) Place Transwell insert (cell side facing up) onto Mowiol
   d) Place coverslip on top of Transwell insert
   e) Mount NC coverslips on 4 µL Mowiol (with cell side facing down)

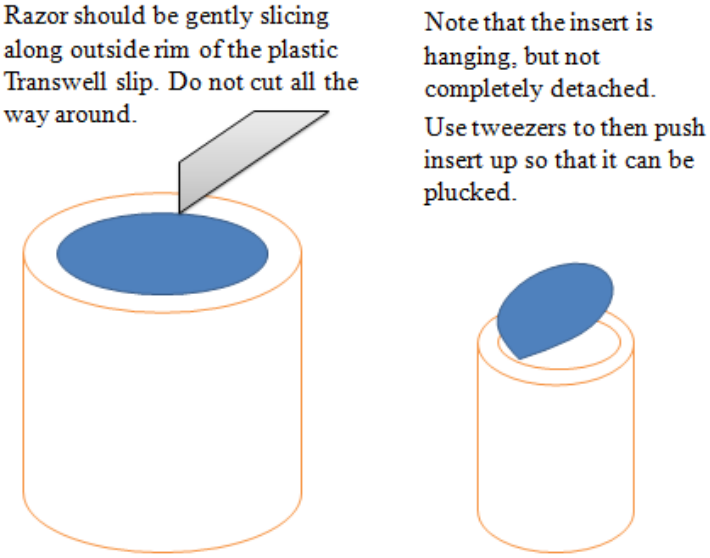

Mounting Transwell on slide:

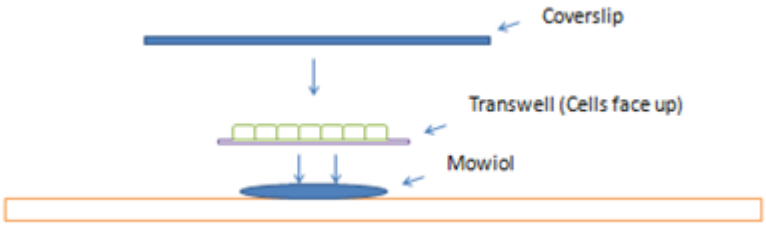

Protocol for analyzing cell morphology in ImageJ:

1) Open ImageJ, File - Open image to analyze
2) Go to Analyze - Set Measurements, check: Area, Feret Diameter, Shape descriptors, Add to overlay. Everything else can be left unchecked.
3) Go to Analyze - Set Scale, for 60x pictures: Distance in pixels- 1, Known distance 0.1075. Set Unit of length to microns, and check Global so you don't have to repeat this for every picture
4) To give the image a scale bar click Analyze – Tools - Scale bar
5) Select Freehand Selections (Bean shaped Icon on the toolbar)
6) Manually trace the shape of a cell
7) Click Analyze - Measure (Ctrl+M), a Results window will pop up, you will want to keep track of this. Specifically, the main parameters of importance are Area, Circ. (circularity), and Feret. The other ones that show up in the table can be left out when organizing data.
8) Repeat until you have all of your desired measurements for the picture. Save the labelled image as a new picture so you can keep an original unedited copy of the image.
9) Once you have finished measuring all your images, you can simply export the results by saving it as a spreadsheet.
10) Keep each condition in a separate results tab, making sure to close the previous tab when going on to the next trial.

Measuring Cell Gap: (do this separately from the cell tracing as not to clutter up your Results tab)

1) Select the Straight line icon on the toolbar
2) Find what you think is the largest gap in between any two adjacent/connected/nearby cells (use your judgment)
3) Click Analyze - Measure, the gap will be shown as 'Length' in the Results tab
4) Repeat until you have your desired measurements, save, and export your results.

Quantifying Results

Take the four parameters and compile them into one spreadsheet, calculate mean, standard deviation and standard error for all of them. Then, use a two-tailed t-test to see whether there are significant differences between the control and the experimental groups, as well as between the experimental groups.

D. Western-Blot Detailed Monocellular Model Protocol

DAY 1:

1) Prepare RIPA buffer
    a) 6 mL RIPA stock solution (PIERCE biotechnologies)
    b) 60 µL EDTA
    c) 60 µL Protease inhibitor [will end up being a 1:100 dilution]
2) Take cells out of incubator, rinse 2x in cold RPMI
    a) 500µL in 24 well plate, 1mL in 6 well plate and Transwell
3) Add H2O2, wait 30 min, rinse again with 2x cold RPMI as above
    a) 300µL in 24 well plate, 1mL in 6 well plate and Transwell
4) Add RIPA buffer to each well, let sit on ice for 5 min
    a) 300µL in 24 well plate, 1mL in 6 well plate or Transwell
    b) While you're waiting, put 3 Eppendorf tubes in the ice as well
5) Use pipette tip or sterile cell scraper to scrape cells off the cover slip
6) Collect all the liquid (combination of fluid and cell fragments), put into LABELED eppendorf tubes
7) Vortex at highest setting
8) Put tubes in ice for 30 min
    a) While this is happening, precool the centrifuge to 4 degrees Celsius
9) Spin the samples in the CHILLED centrifuge for 15 min at 13.3g
10) Collect supernatant solution (about 400µL worth should be plenty) into separate, labeled centrifuge tubes
    a) Be careful not to mix these tubes up with the ones we filled earlier
11) Do Bradford assay (wavelength = 595nm)
    a) Grab 18 cuvettes (for blank, BSA standards, samples, two cuvettes per sample)
        i) BSA concentrations: 5 mM, 2.5 mM, 1.25 mM, .625 mM, 0 mM
    b) Cuvettes include:
        i) 1mL Bradford reagent (Biorad Quick Start Bradford Protein Assay)
        ii) 2µL BSA or sample
            (1) For the 0mM BSA standard, use 2µL of PBS
        iii) Blanks - 1mL PBS
    c) Load identical samples right next to each other into the spectrometer, like the 5mM BSA samples are next to each other, then the 2.5mM samples, and so on
12) Take averages of identical samples, create a standard curve (x axis = concentration, y axis = absorbance)
13) Find what the concentrations of our samples would be, given the absorbances
14) Store sample in the small box labeled "Gemstone Western Blot Samples" in the -20 degree fridge

DAY 2:

15) Grab the bottle of Laemmli buffer from the -20C fridge (it's a big blue bottle, or the small centrifuge tubes labeled Laemmli buffer in the "Restriction Enzymes" box), put it in a bucket of water to let it thaw. Also grab the lysates from the box (white freezer) and let that thaw too.
16) Preheat dry heating block to 70 degrees C

17) Based on the concentration of the lysate and the amount of protein desired per well (preferably around 20 µg, but it really depends on the protein, check the info sheet), figure out how much of the lysate you would need to get that amount of protein.
    a) If more protein needed - add more lysate in (only up to ~30µL, need room for buffer)
    b) If less protein needed - dilute with PBS
18) Into an eppendorf tube, add amount of lysate needed to get desired protein amount. Also add an identical amount of Laemmli buffer, and 1/10th the total volume's amount of Biorad Cleland's Reagent (DTT)
    a) If you have 20µL of lysate and 20µL of buffer (40µL total), add in 4.0µL of DTT
19) Vortex, let sit in dry heating block for 10 min, vortex again
20) Prepare 4-15% gel
    a) Use a razor blade to cut the bottom strip off the gel
21) Grab the electrophoresis cassette and tub. On one side, put the gel with the THIN SIDE facing INWARDS. On the other side, put glass plates
    a) Make sure the glass plates create a seal that is tight as possible
22) Add 1x running buffer to the top of the inner chamber (1x running buffer = 1:10 ratio of BioRad Running Buffer concentrate [with SDS] to deionized water). Add rest of running buffer to outside chamber
23) Add 5µL of protein standard to the far right side of the gel. (Thermo Scientific PageRuler Plus Prestained Protein Ladder)
    a) The order when loading is REVERSED - so if you want your sample to be on the left of the gel, load it in the right wells
    b) Add the protein ladder to the right side of the gel, so it will show up on the left
24) Add samples with the ultrafine pipette tips near the western blot cassettes
    a) Each well holds about 45µL - so load this much of sample
        i) If there is some left - you can start electrophoresis, wait for the wells to go down a bit, and add more sample
            (1) BE CAREFUL WITH THIS - you can't let the sample to get too far down the gel - it can only get as far as the stacking part of the gel
    b) BE CAREFUL NOT TO PUNCTURE THE GEL- don't stab the gel with the pipette- be gentle
25) Start electrophoresis at 80V (25 mA)
    a) Bubbles forming from the whiteish wire at the bottom of the apparatus- means that it's working
    b) This is when you can pause and add more sample if you need to
26) Run at 80V for 1.5 hrs
27) While this is happening - put transfer buffer in the -20 Freezer
    a) Transfer buffer - 350 mL deionized water, 100 mL methanol, 50 mL Biorad Running buffer concentrate (without SDS)
28) Fill up one 45 mL Falcon tube and the white bucket (found where the electrophoresis cassettes are) up with methanol (found in the safe next to the door) - put in -80C freezer
29) When an hour and a half is up, cut a PVDF membrane (Pall Corporation) to about the size of a gel (use the white pad that came with the gel as a guideline)

    a) Be careful not to touch the actual membrane - the oils from your fingers will dirty the blot
30) Take the Falcon tubes and bucket of methanol out of the -80 freezer (NOTE - this hurts to touch, be careful taking it out and do not spill)
31) Take one of the Falcon tubes, pour out the methanol into one of the blue tip covers
32) Using FORCEPS, put the PVDF membrane into the methanol. Let soak for at least a minute
    a) ALWAYS use forceps to handle PVDF membrane
33) Take membrane out of methanol, let equilibrate in cold transfer buffer for 10 min
34) Stop and drain electrophoresis apparatus (you can reuse the running buffer, so put it back into the bottle)
    a) Pry the plastic off to expose the gel - do not rip it
35) Get the clear tray with the spigot on the side, fill up with deionized water, open the cassette on the gel, put the gel facedown into the water
36) Use the spigot to drain the water
37) Add cold transfer buffer to the gel, let sit for 5 minutes to equilibrate
38) Pre rinse 4 filter pads and 4 filter papers (BioRad) in transfer buffer
39) Cut a notch in the upper left side in both the gel and membrane to signify upper left side
    a) Remember that the left side will most likely have the ladder closest to it
40) Take the black/clear cassette, put the black side down and add in this order: pad, paper, gel, membrane, paper, pad
    a) Align cut corners on the gel and membrane
        i) It helps sometimes to use both of the papers to help position the gel on one of the papers
    b) The membrane should be closer to the clear side, the gel should be closer to the black side.
41) Take a second cassette, do the same order, but without the gel and membrane (pad, paper, paper, pad)
42) Put cassettes in apparatus
    a) Black sides of cassettes should be facing the black side of the apparatus
43) Add the frozen methanol bucket to the back of the apparatus
44) Add 2 inches of cold transfer buffer to the container
45) Let run at 100V for 1hr.
46) When you get about 5 min out, prepare 5% milk solution (2.5g powdered Carnation instant milk in 50mL PBS-T)
    a) PBS-T made by mixing 500µL Tween-20 with 500mL 1x unsalted PBS
47) Pour milk solution into a pipette tip cover
48) Remove membrane, place in this container. Make sure membrane is submerged
49) Incubate in on rocker for 1hr.
50) After incubation, rinse with PBS-T three times (5 minutes each)
51) Prepare 3% milk (1.5g Carnation Instant milk powder in 50mL PBS-T)
52) Add 12 mL of 3% milk to a 15mL Falcon tube. Mix 60µL of EACH primary antibody in
    a) For our purposes, this should be GLUT1 and GAPDH (Santa Cruz Biotechnologies)

b) Both are in the small box in the fridge
c) This is good for a 1:200 dilution

53) Submerge membrane in the antibody/milk solution
a) Let it incubate on rocker in 4 degree room overnight
b) NEVER LET MEMBRANE DRY OUT - keep it moist at all times
c) Put saran wrap over the blox with membrane - keeps it from drying out

DAY 3:

54) Wash membrane in PBS-T 6x, 5 min washes each time
55) Prepare second antibody milk solution
a) 3 μL each secondary antibody in 15mL 3%milk (both secondaries GE)
i) 1.5 g of 3% milk powder
ii) 15 mL of PBS-T
b) You need a secondary antibody for EACH primary antibody you add that is from a different animal (We have anti-rabbit and anti-mouse in the lab)
i) GLUT1 anti mouse is 1:30,000 (so 3 microliters antibody into 15microliters pbs and then 3microliters of that into 15ml 3%milk)
ii) GAPDH anti rabbit is 1:1000 (so 3microliters antibody into the 15ml 3% milk)
56) Submerge membrane in the secondary antibody solution, let sit on rocker for 1 hr.
57) During this time, go to dark room and follow manufacturer's instructions to turn on
58) Repeat Day 3, step 1
a) Drain any excess PBS by touching a Kimwipe to the very corner
59) Prepare ECL detection solution - follow manufacturer's instuctions (1mL of Solution A and Solution B) (GE Amersham ECL Prime Western Blotting Detection Reagent)
60) Pipette the ECL solution so that it covers the entire membrane
a) Let sit for 5 minutes
61) Drain excess ECL with Kimwipe, wrap membrane in Saran Wrap
a) Be careful to not get any bubbles on membrane, use a credit card to smooth out
62) Place membrane up in X-ray console, with proteins up (the notch on the upper left side
63) Go to dark room, WITH ONLY THE INFRARED LIGHT ON, open the package of film, place two on top of the membrane. Close up the x-ray console
a) Notch should be on top left side (This is so the emulsion side is facing the membrane)
64) Wait for 1.5 min
a) This waiting time is a lot of trial and error - I've found that a 1.5 min wait period would overexpose the bottom piece of film, but the top piece of film gives a solid picture
i) Film is Kodak Biofilm, single emulsion
b) If it's too exposed, decrease exposure time time, if it's not exposed, increase exposure time.
65) Put the film in the machine, one piece at a time
a) Once you hear the machine "beep," then you can put another piece of film in
b) The film paper is photosensitive, so do not expose the film to the light. When the film is out, only turn on the infrared light.

E. Localization Detailed Monocellular Model Protocol

1) Prepare 5mM H_2O_2
   a) To make 10mL 20x = 9898 µL PBS (20x)+ 102 µL stock H_2O_2
   b) To make desired 5mM = 9500 µL basal media (non-sterile RPMI) + 500 µL H_2O_2 (20x)
2) Prepare Titron (for permeabilizing) - 0.2% Titron in PBS(-). To prepare: 40 µL Titron stock in 20mL PBS(-)
3) Dilute both primary and secondary antibody into 1% BSA-PBS (1:200 dilution)
   a) Weight out 0.1g BSA, Mix into 10mL PBS(-)
   b) 20 µL of either antibody into 4mL BSA-PBS
4) Vacuum out media from cell culture, treat with 300 µL of [h2o2] for 15 minutes
5) Wash with warm basal media 2x (1mL per well)
6) Add 300 µL per well 2% PFA in PBS
7) Incubate for 15 minutes at room temperature
8) Wash 2x with non-salted PBS
9) Add 300 µL Triton per well
10) Incubate 15 minutes at room temperature
11) Wash with non-salted PBS
12) Add 250 µL primary antibody per well (as per dilution in step 3)
13) Incubate overnight at 4 degreees C
14) Wash 2x with unsalted PBS
15) Add 250 µL secondary antibody, incubate for 30 minutes
16) Wash 2x with non-salted PBS
17) Add 100 µL DAPI 1:2000 dilution directly on top of cover slip
18) Add 1 mL non-salted PBS, aspirate out, add another 1mL non-salted PBS
19) Add 5 µL Mowiol per cover slip
20) Mount on slide

Mounting regularly on slide:

F. Localization Detailed Transwell Model Protocol

Using 24 well plates, with 0.4 micron pore size Transwell inserts

HBMECs and ACs attached to apical side of Transwell (only one cell type per Transwell)

- 2 wells containing healthy neurons + Transwells w/ HBMECs
- 2 wells containing injured neurons + Transwells w/ HBMECs
- 2 wells containing healthy neurons + Transwells w/ ACs
- 2 wells containing injured neurons + Transwells w/ ACs

DAY 1:

1) Separate Transwells from the neuron wells and move them to wells containing 300 µL warm RPMI (37 C).
2) Wash wells containing neurons with filtered RPMI (300 µL/well)
3) Add 300 µL warm 5mM H2O2 (in RPMI) to neuron wells (injured condition). Add 300 µL warm RPMI to the other neuron wells (control condition)
4) Incubate for 15 minutes at 37 C
5) Drain H2O2, wash neurons using warm filtered RPMI (300 µL/well)
6) Drain, add 700 µL complete cell media to neuron wells.
7) Place the Transwells back in the same well as the neurons
8) Incubate for ? hours at 37 C [time to be determined at 1 hr, 5 hr or 24 hr]
9) Drain media from Transwells and wells, wash with PBS(+) (300 µL/ Transwell and 300 µL/well)
10) Add cold 2% PFA (300 µL/Transwell and 300 µL/well)
11) Incubate @ RT for 15 min.
12) Drain PFA, then wash w/ PBS(-) (300 µL/ Transwell and 300 µL/ well)
13) Add 0.2% Triton 200 µL/Transwell, 500 µL/ well
14) Incubate @RT for 15 min.
15) Drain Triton, then wash PBS(-) (300 µL/Transwell, 300 µL/well)
16) Block both conditions w/ 1% BSA-PBS for 1 hr @ 4 C (200 µL /Transwell, 300 µL/ well)
    a) For 1% BSA-PBS
17) Weigh 0.1g BSA, mix into 10ml of PBS(-)
18) Wash w/ PBS(-) (300 µL/ Transwell and 300 µL/ well)
19) Add mouse anti-human GLUT1 primary antibody (200 µL /Transwell and 300 µL/well)
    a) For 1 µg/ml (primary/secondary) antibody dye
        i) Take 4 mL 1% BSA-PBS, add 20 µL of primary or secondary antibody
20) Leave overnight @ 4C

DAY 2:

1) Wash w/ PBS(-) (wait 5 min.) (300 µL/ Transwell and 300 µL/ well)
2) Add FITC-conjugated goat anti-mouse secondary antibodies 250 µL /Transwell and 500 µL to well
3) Incubate 1 hr. in DARK @RT
4) Wash w/ PBS(-) (wait 5 min.) (300 µL/ Transwell and 300 µL/ well)
5) Add 1:2000 DAPI (100 µL/ Transwell and well)
6) Incubate 3 min @RT
7) Wash w/ PBS(-) (300 µL/ Transwell and 300 µL/ well)
8) Mount on slide

a) Use a razor blade to cut out the cell insert on the Transwell
b) Place 4 µL Mowiol on slide
c) Place Transwell insert (cell side facing up) onto Mowiol
d) Place coverslip on top of Transwell insert
e) Mount neuron coverslips on 4 µL Mowiol (with cell side facing down)

Razor should be gently slicing along outside rim of the plastic Transwell slip. Do not cut all the way around.

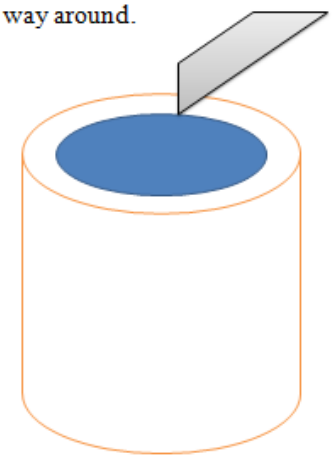

Note that the insert is hanging, but not completely detached.

Use tweezers to then push insert up so that it can be plucked.

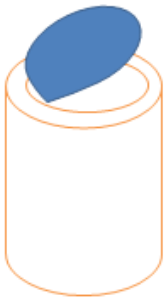

Mounting Transwell on slide:

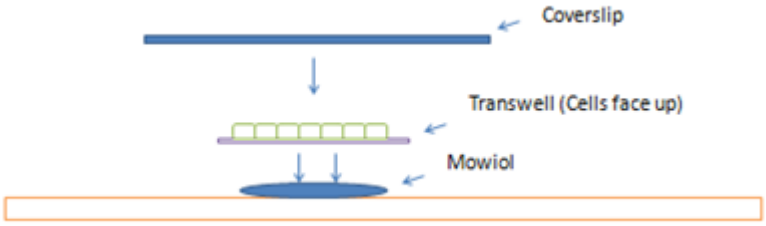

G. Cell Viability Detailed Monocellular Model Protocol

After removing cells from incubator:

1) Wash cells 1x w/ warm RPMI (1 mL)
2) Add 300 µL phenol red free RPMI to control wells
3) Add 300 µL 5mM H2O2 to injured wells
   a) 1st dilution (100mM H2O2) : 9898 µL PBS + 102 µL stock H2O2 (9.82 M)
   b) 2nd dilution: 9500 µL PBS + 500 µL of (100mM H2O2) = 10 mL of 5mM H2O2
4) Incubate for 15 min. @ 37 Celsius in non-sterile incubator
5) Wash cells 1x w/ warm RPMI (1 mL).
6) Add 300 µL of live-dead dye in PBS to each well (0.1µM calcien, 1µM ethidium homodimer)
   a) 1st dilution (0.04mM calcien): 99 µL PBS + 1µL stock calcien (4mM)
   b) 2nd dilution: 12.5 µL of (0.04mM calcien) + 2.5 µL stock ethidium (2mM) + 4895 µL PBS = 5mL 0.1µM calcien and 1µM ethidium
7) Incubate for 15 min. @ 37 Celsius.
8) Wash cells 1x w/ warm PBS (1 mL)
9) Fix cells w/ 300 µL PFA for 15 min. @ RT
10) Wash cells 1x w/ PBS (1 mL)
11) Mount on slide

Mounting regularly on slide:

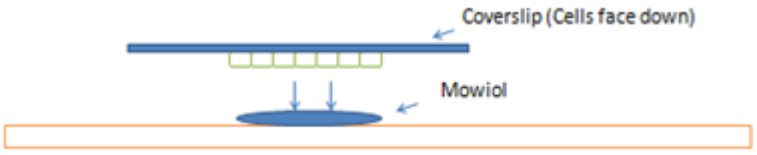

H. Viability Detailed Transwell Model Protocol

1) Wash neurons with 1mL warm complete cell media
2) Take Transwell insert out of neuron well, place it in another well containing 700 µL complete cell media
3) Add 300 µL 5mM H_2O_2 to injured condition wells. Add 300 µL warm RPMI to control condition wells
4) Incubate 15 min @ 37 degrees Celsius
5) Wash in the same manner as step 1
6) Put Transwells back into neuron wells, incubate at 37 degrees Celsius for 1 hour [and later 5 hours, 24 hours]
7) Drain and move transwell into an empty well.
8) Add 100 µL of 0.25% Trypsin to the transwell and neuron well.
9) Incubate the plate for 5 minutes
10) Collect the Trypsinized solution in a falcon tube and resuspend the cells in 900 µL of RPMI
11) Centrifuge the falcon tubes for 5 minutes at 1500 rpm
12) Aspirate the media
13) Resuspend the pellet in 50 µL of RPMI and 50 µL of trypan blue
14) Place 10 µL of the solution in the hemocytometer
15) Look at the cells under the light microscope and count the number of viable cells per the instruction on the hemocytometer